

# Stabilized QFT: verification supplement

C. D. Chlouber  
Houston, USA\*  
(Dated: 03/14/21)

This paper does two things: (1) it recaps the method of stabilized amplitudes that resolves divergence issues in QFT without infinite charge and mass renormalizations, and (2) it presents a detailed case study which verifies that stabilized amplitudes agree with renormalization for radiative corrections in Abelian and non-Abelian gauge theories.

## I. INTRODUCTION

In a companion paper [4], we argue that action of elementary charges on the vacuum leads to finite amplitudes for radiative corrections without infinite mass, charge, and wave-field renormalizations: It was determined that renormalization is only required in the standard (unstabilized) theory because it violates the law of conservation of energy; in this connection, it does not account for all intermediate mass states dressed with vacuum energy. Renormalization attempts to fix the problem by redefining mass and charge, but this solution misses the underlying physics and renders the theory more complex than necessary.

The main purpose of this paper is to show that the stability method agrees with renormalization theory and therefore with experiment for specific radiative corrections in quantum field theory (QFT). After a brief summary of the rationale and rules for constructing stabilized amplitudes, we verify in detail that net S-matrix corrections in QED are finite and agree with renormalization theory to all orders in perturbation theory; finally, we verify the method for one-loop diagrams in QCD and electroweak theories. Standard Model nomenclature is defined in Appendix A.

## II. STABILITY THEORY

### A. Physical model

Conservation of energy requires that an electrical or color charge redistribute vacuum energy into positive and negative energy parts such that its net energy

$$\mathcal{E}^+ + \mathcal{E}^- = 0 \quad (1)$$

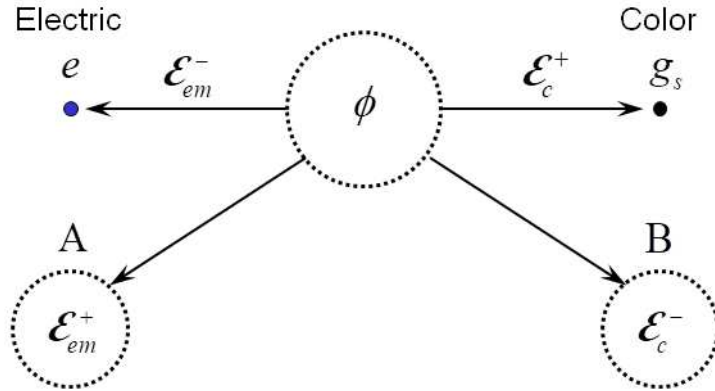


Figure 1. Intrinsically stable electrical and color charges  $\{e, g_s\}$  effectively draw  $\{\text{negative, positive}\}$  energy from the vacuum  $\phi$  leaving an energy  $\{\text{surplus, deficit}\}$  in surrounding (far-field) regions  $\{A, B\}$ .

\* chlouber@hepir.net

remains zero. Actions of elementary charges on vacuum  $\phi$  are depicted in Fig. 1. For complex irreducible scattering processes, the model in Fig. 1 suggests there exists point-like, near-field contributions to scattering amplitudes in addition to those associated with unrenormalized (core) amplitudes in surrounding regions.

For an electron of mass  $m$ , vacuum polarization effectively spreads the charge out [51] over a subregion of the far-field having spacial extent approximated by the Compton wavelength  $\lambda_c = 1/m$ . From (1), the self-energy [10]

$$m_{em}^+ = \frac{3\alpha m}{2\pi} \left( \ln \frac{\Lambda_o}{m} + \frac{1}{4} \right) \quad (2)$$

is paired with a deficit  $m_{em}^-$  to give a stability condition

$$m_{em}^+ + m_{em}^- = 0, \quad (3)$$

where  $\alpha$  is the fine structure constant, and  $\Lambda_o$  is a cutoff. We can model the deficit as an interaction between the observed charge  $-e$  and a vacuum potential  $\phi_{vac} > 0$  which acts on the charge akin to a spherical capacitor depicted in Fig. 2, where the radius of the near-field (vacuum depletion) region is comparable to the Compton wavelength of the electromagnetic mass:  $\lambda_c^{em} = 1/m_{em}^+$ . Considering (3), the net mass-energy of a charged fermion is just the observed core mechanical mass  $m$  generated by the Higgs field interaction in electroweak theory. Using mass formula (A12), the vacuum potential can be related to a displacement of the vacuum from the ground state

$$\phi_{vac} = \frac{\eta}{e} g_e \langle 0 | \Phi | 0 \rangle, \quad (4)$$

where  $\eta \equiv \lambda_c / \lambda_c^{em} \gg 1$  is a scale parameter, and  $g_e$  is the coupling of the electron field  $\psi$  to the Higgs field  $\Phi$ . In contrast to Poincaré's theory [34], wherein internal non-electromagnetic stresses hold a charge together, here an elementary charge is presumed stable, and the external vacuum potential well stabilizes the system.

An electron in the potential well of Fig. 2 is dressed with negative electromagnetic energy in the near-field and positive energy in the far-field. In the renormalization approach, one starts with a bare electron

$$m_o \equiv m - e\phi_{vac}, \quad (5)$$

self-interaction dresses it with positive electromagnetic energy  $m_{em}^+$ , and the renormalization condition

$$m_o + m_{em}^+ = m \quad (6)$$

is subsequently applied to redefine the mass and thereby conserve energy. However, from the energy conservation model in Fig. 1,  $m_{em}^+$  and  $m_{em}^-$  are always present, the total mass reduces to the observed mass, and there should be no need to introduce unobservable bare quantities for either mass or charge.

If we insist on using physically measured values for mass and charge from the start, then we only need to determine near-field scattering amplitude corrections that manifestly conserve energy and result in an energy deficit or surplus for electroweak or strong interactions, respectively: This involves accounting for the additional mass states implied by (3). Considering all changes in vacuum energy, a complete set of mass states can be defined, and we can formulate a finite theory of radiative corrections that includes all possible intermediate states, and no asymmetry such as (5), necessitating a redefinition of mass or charge, is introduced.

## B. Dressed mass states

This section generalizes the model in Fig. 1 to fermion (FSE) and boson (BSE) self-energy processes involving electroweak interactions. General rules for dressing a particle with vacuum energy are given.

External lines for processes in Fig. 3 involve (a) gauge bosons  $b \in \{\gamma, W, Z, H\}$ , and (b,c) fermions  $f \in \{j\sigma\}$  corresponding to family  $j$  with component index  $\sigma = \pm$ . Blobs in Fig. 3 contain irreducible insertions, which in general, may involve other particles in the Standard Model mass set

$$\mathbb{M} = \{m_f, m_W, m_Z, m_H\} .$$

On the mass shell, scattering amplitudes  $\Sigma^f(p)$  and  $\Sigma^b(k^2)$ , given in Appendix E, define fermion and boson self-energy functions [19, 44]

$$M_f = \Sigma^f(p) \Big|_{\not{p}=m_f} \text{ and} \quad (7)$$

$$M_b^2 = \text{Re} [\Sigma^b(k^2)]_{k^2=m_b^2} . \quad (8)$$

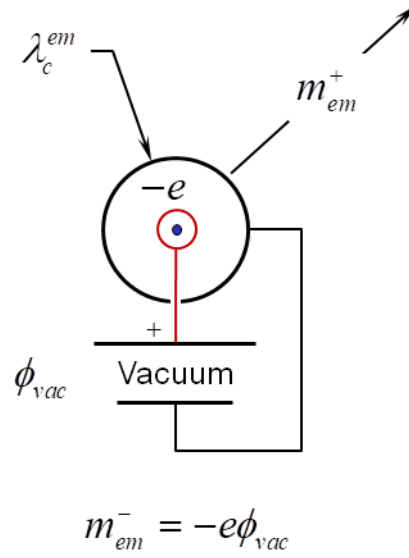


Figure 2. Effective vacuum potential due to vacuum depletion acts on an electron charge similarly to spherical capacitor. Since stability requires  $m_{em}^+ - e\phi_{vac} = 0$ , the total energy of the electron in the well and dressed in its electromagnetic field is just its observed mass-energy. For a positron  $\phi_{vac} < 0$ .

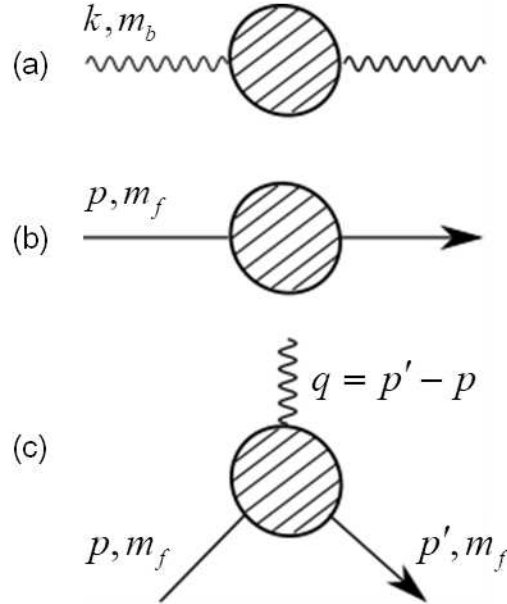


Figure 3. Generic self-energy and vertex diagrams: (a) BSE, (b) FSE, and (c) vertex.

Physically,  $M_f$  and  $M_b$  each represent energy borrowed from the vacuum in a near-field region of radius

$$r_o \simeq \lambda_c (M_f | M_b)$$

to create a configuration of high-energy virtual particles in a far-field region:  $r > r_o$ . In order to have well defined amplitudes for FSE and BSE processes, there must exist corresponding negative probability (depletion) amplitudes that oppose (7) and (8), thereby ensuring conservation of energy. Loosely, one may think of (8) as a squared energy borrowed from the vacuum and  $-M_b^2$  as the deficit. Depletion amplitudes involve two additional mass levels indexed by  $\lambda = \pm 1$ , where core masses,  $m_f$  or  $m_b$ , are dressed with positive and negative vacuum energy.

Allowed dressed core mass (DCM) levels for fermions in FSE processes and bosons in BSE processes are defined by requiring that averages of free field Lagrangian densities, Yukawa (A11) and Higgs (A6), over dressed mass levels

$\lambda = \pm 1$  are stationary: By inspection,  $\mathcal{L}_F(m_f \rightarrow m_f + \lambda M_f)$  and  $\mathcal{L}_H(m_b^2 \rightarrow m_b^2 + \lambda M_b^2)$  meet this requirement.

To ensure consistency when fermions and bosons mix in FSE and BSE processes, dressed mass levels for all  $m \in \mathbb{M}$  in the blobs of Fig. 3 are defined by the replacement

$$m^n \rightarrow m^n (1 + \lambda \eta^n) , \quad (9)$$

where  $\eta$  is a common scaling factor:  $M_f = \eta m_f$  and  $M_b = \eta m_b$ , and

$$n = \begin{cases} 1 & \text{FSE/vertex} \\ 2 & \text{BSE} \end{cases} \quad (10)$$

for irreducible FSE, vertex, and BSE diagrams in electroweak theory.

Taking into account the fermion mass formula (A12), the DCM rule

$$m_f \rightarrow m_f (1 + \lambda \eta) \quad (11)$$

for fermions in FSE processes corresponds to a vacuum fluctuation ( $h \neq 0$ )

$$\Delta v = \lambda \eta v , \quad (12)$$

where the ground state energy  $v$  is determined from (A10). For selected  $\lambda$  and  $\eta$ , the displacement (12) is the same for all charged fermions.

For bosons in BSE processes,

$$m_b^2 \rightarrow m_b^2 (1 + \lambda \eta^2) . \quad (13)$$

Since  $m_b \propto v$  from (A7)-(A9), the boson vacuum is shifted  $v^2 \rightarrow v^2 + \Delta v^2$  with

$$\Delta v^2 = \lambda \eta^2 v^2 . \quad (14)$$

For external particles in Fig. 3, dressed momenta in the blobs are:

$$p_d = m_f (1 + \lambda \eta) + \delta p_{os} , \quad (15)$$

$$k_d^2 = m_b^2 (1 + \lambda \eta^2) + \delta k_{os}^2 , \quad (16)$$

where  $\delta p_{os}$  and  $\delta k_{os}^2$  are off-shell terms.

Vertex factors (A13)-(A15), including the weak mixing angle (A5), charge (A16), and neutral current coupling constants (A17) are all stationary under (9). However, propagators (A18)-(A20) involving massive particles are not stationary under DCM transforms, and dressed amplitudes (18) constructed from them are either driven to zero or a stabilizing correction for finite tree or divergent loop processes, respectively.

### C. Scattering amplitude

Generally, if an irreducible radiative process represented by  $\Omega$  borrows energy from the vacuum creating a deficit, then an opposing amplitude is required to ensure conservation of probability and energy. For the moment, assume dimensional regularization is used to tame improper integrals. To account for the deficit and include all possible intermediate mass states, the total scattering amplitude for electroweak interactions is defined by

$$\hat{\Omega} = \Omega(\mathbb{M}) - \overline{\Omega}(\mathbb{M}) , \quad (17)$$

where  $\Omega$  accounts for self-interaction effects involving physical masses in  $\mathbb{M}$ , and

$$\overline{\Omega}(\mathbb{M}) = \frac{1}{2} \lim_{\eta \rightarrow \infty} \sum_{\lambda=\pm 1} \Omega(\mathbb{M}_d = \eta_\lambda \mathbb{M}) \quad (18)$$

is a subtrahend for vacuum depletion; from (9), we have

$$\eta_\lambda \equiv \begin{cases} 1 + \lambda \eta & \text{FSE/vertex} \\ \sqrt{1 + \lambda \eta^2} & \text{BSE} \end{cases} . \quad (19)$$

For any  $m \in \mathbb{M}$ , the dressed mass is

$$m_d = \eta_\lambda m. \quad (20)$$

If an energy cutoff  $\Lambda_o$  is assumed in lieu of dimensional regularization, then we must include  $\Lambda_o$  in the argument set of  $\Omega$ . The cutoff scales in the same way as (20); that is,

$$\Lambda_d \equiv \eta_\lambda \Lambda_o. \quad (21)$$

In addition to  $m_b$  or  $m_f$ ,  $\Omega$  depends on external momenta  $\{k, p\}$  for Feynman diagrams in Fig. 3 which may be on- or off-shell. For notational simplicity, any dependence on external momentum parameters has been suppressed during construction of  $\overline{\Omega}$  because  $\{k, p, q\}$  are implicitly dependent on associated core masses.

Since the positive and negative energy regions in Fig. 1 for color charges are interchanged relative to electrical charges, the stabilized amplitude in QCD is given by

$$\hat{\Omega}_{QCD} = \lambda_s \hat{\Omega}, \quad (22)$$

where  $\hat{\Omega}$  from (17) employs the usual Feynman rules, and

$$\lambda_s = -1 \quad (23)$$

is a switching factor.

### III. VERIFICATION

This section justifies rules (17) and (22) for computing stabilized amplitudes.

In Appendix B, we evaluate divergent integrals in  $\overline{\Omega}$  for dressed mass states in Feynman diagrams, and show how they reduce to mass shell renormalization conditions.

For Abelian QED in Appendix C, stabilized amplitudes agree with renormalization theory for vacuum polarization, fermion self-energy, and vertex processes to all orders in perturbation theory. Accounting for vacuum depletion eliminates all divergences: In particular, opposing currents associated with dressed fermion states stabilize the photon self-energy without charge renormalization, and neither mass nor wave field renormalization is required for the fermion self-energy.

For non-Abelian QCD in Appendix D, we apply the stability method to a collection of one-loop diagrams using a modified renormalization formula to derive an effective color charge (D12) and running coupling constant (D23) with an energy scale signature consistent with QCD's prediction of asymptotic freedom [15, 36] and its agreement with experimental results [7]. However, the crucial difference is that finite stabilization parameters replace infinite renormalization constants. The results show that the switching factor  $\lambda_s = -1$  in (D12) is essential; physically, this means that dressed particles in  $\overline{\Omega}$  are associated with positive energy in the near-field, and physical masses in the depletion part  $-\Omega$  are cloaked in negative energy. Also, an analytical expression for the reference mass  $M_s$  in QCD is derived which gives  $M_s = 70.65 \text{ GeV}/c^2$ ; see (D27).

Generally, fundamental couplings are well defined only on the mass shell, where bosons mediating the interaction are free, and stabilized boson self-energy functions vanish; therefore, the elementary charge used in the Feynman rules is a rock-solid constant. An effective running coupling includes energy dependent vacuum polarization effects for screening or anti-screening, which can otherwise can be associated with modifications to field propagation functions.

For one-loop electroweak corrections in Appendix E, we verify that stabilized boson self-energy corrections including  $\Delta r$ , fermion self-energies, and vertex processes are finite and agree with renormalization [6, 19]. Electroweak depletion amplitudes for boson and fermion self-energy processes are reduced by expanding core amplitudes in a Taylor series and applying (18): The resulting stabilized amplitudes (E12) and (E37) are unique and yield stability conditions that agree with only one renormalization scheme. While the electrical charge (A16) is invariable according to (E27), couplings  $\{g_W^2, g_Z^2\}$  and  $\theta_W$  can vary due to finite on-shell mass shifts  $\{\delta m_W^2, \delta m_Z^2\}$  derived from stabilized  $W$ - and  $Z$ -boson self-energy corrections; see (E48) and (E49). Therefore, resulting  $\Delta r$  corrections (E28) to BSE amplitudes for  $W$ - and  $Z$ -bosons are a simple consequence of the constancy of the electrical charge, a stability result. Finally, we verify that muon decay with  $\Delta r$  corrections yields expected results without renormalization.

For non-Abelian electroweak and QCD theories, the stability method is expected to yield finite results to all orders in perturbation theory since it is applied to each irreducible radiative correction in any complex Feynman diagram.

Numerical results are presented in Appendix F for electroweak boson and fermion self-energy profiles. Stabilized results for  $\gamma - Z$  mixing,  $Z$ -boson, and  $W$ -boson polarization profiles differ from and update those given in [2, 19].

## Appendix A: Standard Model nomenclature

This appendix summarizes required machinery of the Standard Model utilizing references [19, 33]. Natural units are assumed; that is,  $\hbar = c = 1$ .

### 1. Electroweak theory

The electroweak Lagrangian

$$\mathcal{L}_{EW} = \mathcal{L}_G + \mathcal{L}_H + \mathcal{L}_F \quad (\text{A1})$$

for the physical particles includes gauge, Higgs, and fermion parts. Gauge fixing and ghost terms are omitted in (A1) since it is only necessary to consider physical particles for this development. The gauge part, based on a Yang-Mills prototype (A22), is given by

$$\mathcal{L}_G = -\frac{1}{4}W_{\mu\nu}^a W^{a,\mu\nu} - \frac{1}{4}B_{\mu\nu}B^{\mu\nu},$$

where the field strength tensors

$$\begin{aligned} W_{\mu\nu}^a &= \partial_\mu W_\nu^a - \partial_\nu W_\mu^a + g_W \varepsilon_{abc} W_\mu^b W_\nu^c \text{ and} \\ B_{\mu\nu} &= \partial_\mu B_\nu - \partial_\nu B_\mu \end{aligned} \quad (\text{A2})$$

are expressed in terms of derivatives of the gauge fields: a triplet  $W_\mu^a$ ,  $a = 1, 2, 3$  of vector bosons and a singlet  $B_\mu$  which transform according to  $SU(2)$  and  $U(1)$  symmetry groups [14], respectively. In (A2),  $g_W$  is the non-Abelian  $SU(2)$  gauge coupling constant, and  $\varepsilon_{abc}$  is the Levi-Civita tensor representing the structure constants of  $SU(2)$ .

The Higgs part is given by

$$\mathcal{L}_H = (D_\mu \Phi)^\dagger (D^\mu \Phi) - V(\Phi),$$

where

$$\Phi(x) = \frac{1}{\sqrt{2}} \begin{pmatrix} 0 \\ v + h(x) \end{pmatrix} \quad (\text{A3})$$

is an isospin doublet in a unitary gauge,  $h(x)$  is the real Higgs field which fluctuates about a vacuum  $v = \sqrt{-\frac{\mu_\Phi^2}{\lambda_\Phi}}$ ,

$$V(\Phi) = \mu_\Phi^2 \Phi^\dagger \Phi + \lambda_\Phi (\Phi^\dagger \Phi)^2$$

is the Higgs potential, that with  $\lambda_\Phi > 0$  and  $\mu_\Phi^2 < 0$  for symmetry breaking, leads to the stable ground state (A3). The Higgs doublet  $\Phi$  is coupled to the gauge fields via the covariant derivative

$$D_\mu = \partial_\mu - ig_W T_a W_\mu^a - ig_B \frac{Y}{2} B_\mu,$$

where  $\vec{T} = \vec{\sigma}/2$  are weak isospin generators,  $\vec{\sigma}$  are Pauli matrices satisfying the  $SU(2)$  algebra  $[\sigma_i, \sigma_j] = 2i\varepsilon_{ijk}\sigma_k$ , and  $g_B$  is the Abelian coupling constant.  $\Phi$  carries hypercharge  $Y = Y_\Phi \equiv 1$  and a third component of isospin  $T_3 \Phi = -\frac{1}{2}\Phi$ . In terms of the gauge fields, the physical fields for charged  $W$ -bosons, neutral  $Z$ , and photon  $A_\mu$  are

$$W_\mu^\pm = \frac{1}{\sqrt{2}} (W_\mu^1 \mp W_\mu^2),$$

$$\begin{pmatrix} Z_\mu \\ A_\mu \end{pmatrix} = \begin{pmatrix} \cos \theta_W & \sin \theta_W \\ -\sin \theta_W & \cos \theta_W \end{pmatrix} \begin{pmatrix} W_\mu^3 \\ B_\mu \end{pmatrix}, \quad (\text{A4})$$

where the weak mixing angle  $\theta_W$  is defined by

$$\begin{aligned} \cos \theta_W &= \frac{g_W}{g_Z} \\ &= \frac{m_W}{m_Z}, \end{aligned} \quad (\text{A5})$$

where  $g_Z = \sqrt{g_W^2 + g_B^2}$ . Omitting higher-order non-mass terms, the Higgs part expressed in terms of the physical fields is given by

$$\mathcal{L}_H \simeq \frac{1}{2} \partial_\mu h \partial^\mu h + m_W^2 W_\mu^- W^{+\mu} + \frac{1}{2} m_Z^2 Z_\mu Z^\mu - \frac{1}{2} m_H^2 h^2, \quad (\text{A6})$$

where

$$m_W = \frac{1}{2} g_W v \quad \text{and} \quad (\text{A7})$$

$$m_Z = \frac{1}{2} g_Z v \quad (\text{A8})$$

are vector boson masses generated via the Higgs mechanism [17, 41, 50]. The scalar boson mass (Higgs) is

$$m_H^2 = 2\lambda_\Phi v^2, \quad (\text{A9})$$

where the quartic self-interaction parameter  $\lambda_\Phi$  may be determined using the identity

$$v^2 = \frac{m_W^2 \sin^2 \theta_W}{\sqrt{\pi\alpha}} \quad (\text{A10})$$

and experimental values [47] for  $m_W$ ,  $\sin^2 \theta_W$ , and  $m_H$ .

Suppressing the color attribute for quarks, the fermion part of the Lagrangian is given by

$$\mathcal{L}_F = \sum_j \bar{\psi}_L^j i \gamma^\mu D_\mu \psi_L^j + \sum_{j\sigma} \bar{\psi}_R^{j\sigma} i \gamma^\mu D_\mu \psi_R^{j\sigma} + \mathcal{L}_F^{\text{Yukawa}}$$

for each lepton or quark family ( $j$ ), where  $\gamma^\mu$  are Dirac matrices,

$$\psi_L^j = \begin{pmatrix} \psi_L^{j+} \\ \psi_L^{j-} \end{pmatrix}$$

is a left-handed fermion doublet with component index  $\sigma = \pm$ , and  $\psi_R^{j\sigma}$  is a right-handed singlet for a fermion  $f$  indexed by  $j\sigma$ . The Yukawa interaction part of  $\mathcal{L}_F$  is given by a sum of terms

$$\begin{aligned} \mathcal{L}_F^{\text{Yukawa}}(m_{j\sigma}) &= g_{j\sigma} \left[ \left( \bar{\psi}_L^j \Phi \right) \psi_R^{j\sigma} + \bar{\psi}_R^{j\sigma} \left( \Phi^\dagger \psi_L^j \right) \right] \\ &= -m_{j\sigma} \left[ \bar{\psi}_L^{j-} \psi_R^{j\sigma} + \bar{\psi}_R^{j\sigma} \psi_L^{j-} \right], \end{aligned} \quad (\text{A11})$$

where  $g_{j\sigma}$  are coupling constants, and masses generated from the interaction between the fermion and Higgs fields are

$$m_{j\sigma} = \frac{1}{\sqrt{2}} g_{j\sigma} (v + h) \Big|_{h=0}. \quad (\text{A12})$$

We will also need vertex factors and propagators below for later reference; these, along with propagators for the Higgs, ghost fields, and vertex factors for  $SU(N)$  theories may be found in the literature and [33]. For fermions coupling to the  $W$ ,  $Z$ , and  $\gamma$ ; vertex factors are

$$\begin{array}{c} \text{---} W^\pm \\ \text{---} f \\ \text{---} f' \end{array} = i \frac{e}{\sqrt{2} s_w} \gamma^\mu \frac{1}{2} (1 - \gamma_5), \quad (\text{A13})$$

$$\begin{array}{c} \text{---} Z \\ \text{---} f \\ \text{---} f \end{array} = i e \gamma^\mu (v_f - a_f \gamma_5), \quad (\text{A14})$$

$$\begin{array}{c} \text{---} \gamma \\ \text{---} f \\ \text{---} f \end{array} = i e Q \gamma^\mu, \quad (\text{A15})$$

where ( $f = j\sigma$ ,  $\sigma = \pm$ ,  $f' = j\sigma'$ ,  $\sigma' = \mp$ ), charge operator  $Q$  is defined by the Gell-Mann-Nishijima relation

$$Q = T_3 + \frac{Y}{2}$$

with third component of isospin  $T_3$  and hypercharge  $Y$  specific to the fermion, electrical charge  $e$  satisfies

$$e \equiv g_W \sin \theta_W = g_B \cos \theta_W, \quad (\text{A16})$$

and the vector and axial vector coefficients

$$v_f = \frac{T_3^f - 2s_w^2 Q}{2s_w c_w} \quad \text{and} \quad (\text{A17})$$

$$a_f = \frac{T_3^f}{2s_w c_w}$$

are neutral current (NC) coupling constants with  $\{s_w \equiv \sin \theta_W, c_w \equiv \cos \theta_W\}$ .

The fermion propagator [11] is

$$\frac{\overrightarrow{p}}{f} = S_F(p, m_f) = \frac{i}{\not{p} - m_f + i\varepsilon}, \quad (\text{A18})$$

where  $\not{p} = \gamma^\mu p_\mu$ , and anti-fermions are denoted by  $\bar{f}$ . The vector boson propagator is

$$\alpha \text{---} \underset{\beta}{\sim}^k = D_F^{\alpha\beta}(k) = \frac{-ig^{\alpha\beta}}{k^2 - m_b^2 + i\varepsilon} \quad (\text{A19})$$

in the Feynman-'t Hooft gauge [21], where the metric tensor  $g_{\alpha\beta} = g^{\alpha\beta}$  has non-zero components

$$g_{00} = -g_{11} = -g_{22} = -g_{33} = 1,$$

and  $b \in \{W, Z, \gamma\}$ . For the Higgs, we have

$$\text{---} \overset{k}{\text{---}} = \frac{i}{k^2 - m_H^2 + i\varepsilon}. \quad (\text{A20})$$

Finally, unphysical particles including gauge fixing Higgs  $\{\phi^\pm, \chi\}$  and unitarity preserving Faddeev-Popov ghosts  $\{u^\pm, u^Z, u^\gamma\}$  occur in loop corrections discussed in Appendix E.

## 2. QCD theory

Quantum Chromodynamics is a Yang-Mills theory involving  $n_f = 6$  quarks interacting with  $n_g = 8$  massless gluons. Quarks carry color charge and belong to the fundamental representation of the color group  $G = SU(3)$ , and the gluons are in the adjoint representation  $r = G$ . Omitting gauge fixing and Faddeev-Popov ghost terms, the QCD Lagrangian is

$$\mathcal{L}_{QCD} = \sum_{f=1}^{n_f} \bar{\psi}_f^j \left( i\gamma_\mu D_{jk}^\mu - m_f \delta_{jk} \right) \psi_f^k + \mathcal{L}_{YM}, \quad (\text{A21})$$

$$D_{jk}^\mu = \delta_{jk} \partial^\mu - ig_s \left( \vec{t} \cdot \vec{A}^\mu \right)_{jk},$$

$$\mathcal{L}_{YM} = -\frac{1}{4} F_{\mu\nu}^a F_a^{\mu\nu}, \quad (\text{A22})$$

$$F_{\mu\nu}^a = \partial_\mu A_\nu^a - \partial_\nu A_\mu^a + g_s f^{abc} A_\mu^b A_\nu^c,$$

where  $\psi_f^k$  is a Dirac spinor for the quark field with flavor  $f$  and color state  $k \in \{R, G, B\}$ ,  $g_s$  is the color charge,  $t^a = \lambda^a/2$ ,  $a = 1, \dots, n_g$  are generators represented by  $3 \times 3$  Gell-Mann matrices  $\lambda^a$ ,  $A_\mu^a$  are color-charged gluon fields, and  $f^{abc}$  are structure constants of  $G$ . The t-matrices, which occur in a quark/gluon vertex

$$\begin{array}{c} \text{---}^g \\ | \\ \text{---}^f \end{array} = ig_s \gamma^\mu t^a, \quad (\text{A23})$$



and gluon propagator

$$\underset{a,\mu}{\overset{k}{\sim}}_{b,\nu} = \frac{-ig^{\mu\nu}t^at^b}{k^2 + i\varepsilon} \quad (\text{A24})$$

rotate the quark in color space and generate the Lie algebra for  $G$

$$[t^a, t^b] = if^{abc}t^c.$$

The structure constants occur in three- and four-gauge-boson vertices and satisfy

$$f^{acd}f^{bcd} = C_2(G)\delta^{ab},$$

where  $C_2(G) = N$  is an eigenvalue of the quadratic Casimir operator.

### Appendix B: Divergent integrals

Here we develop integration formulae required for evaluation of stability corrections using cutoff and dimensional regularization. In the  $p$ -representation, loop diagrams involve four-dimensional integrals over momentum space, and the real parts of scattering amplitudes contain integrals of the form [24]

$$D(\Delta) = \frac{1}{i\pi^2} \int \frac{d^4p}{(p^2 - \Delta)^n} = \frac{(-1)^n}{\pi^2} \int \frac{d^4p_\varepsilon}{(p_\varepsilon^2 + \Delta)^n}, \quad (\text{B1})$$

where  $\Delta$  depends on the core mass  $m$ , momentum parameters external to the loop, and integration variables. On the right side of (B1), a Wick rotation has been performed via a change of variables  $p = (ip_\varepsilon^0, \vec{p}_\varepsilon)$ , so that the integration can be performed in Euclidean space where  $p_\varepsilon^2 = p_\varepsilon^0 p_\varepsilon^0 + \vec{p}_\varepsilon \cdot \vec{p}_\varepsilon$ . Integrals for the divergent case ( $n = 2$ ) must be regulated such that they are consistently defined for core and dressed core masses. For  $m$ ,  $D$  is regularized using a cutoff  $\Lambda_\circ$  on  $s = |p_\varepsilon|$ . In four-dimensional polar coordinates, we have

$$D(\Delta, \Lambda_\circ) = \frac{1}{\pi^2} \int d\Omega \int_0^{\Lambda_\circ} ds \frac{s^3}{[s^2 + \Delta]^2}. \quad (\text{B2})$$

For dressed masses,  $\Delta$  depends on  $m_d$ , and the domain of integration in (B2) must be scaled according to (21); consequently, we need to evaluate

$$D_d = D[\Delta(m_d), \Lambda_d].$$

With a change of variables  $s = \eta\lambda t$  and taking the limit  $\eta \rightarrow \infty$ , we obtain

$$D_d = D(\Delta_\circ, \Lambda_\circ), \quad (\text{B3})$$

where

$$\Delta_\circ = \lim_{\eta \rightarrow \infty} \eta\lambda^{-2} \Delta(\eta\lambda m). \quad (\text{B4})$$

For example, the standard divergent integral [24]

$$\begin{aligned} D_\circ &\equiv D(\Delta = m^2, \Lambda_\circ) \\ &= \ln \frac{\Lambda_\circ^2}{m^2} - 1 + O\left(\frac{m^2}{\Lambda_\circ^2}\right) \end{aligned} \quad (\text{B5})$$

is manifestly invariant under scaling rules (20) and (21); that is,

$$D_\circ = D(m_d^2, \Lambda_d). \quad (\text{B6})$$

Note that the average of (2) over dressed masses is stationary due to (B6); this ensures that the FSE in QED is finite as shown in detail in Appendix C2.

In contrast to the cutoff method, dimensional regularization evaluates a Feynman diagram as an analytic function of spacetime dimension  $d$ . For  $n = 2$  and  $d^4p \rightarrow d^d p$  in (B1),  $D$  may be evaluated using [22, 29]

$$\begin{aligned} D(\Delta, \sigma) &= \pi^{-\sigma} \Gamma(\sigma) \Delta^{-\sigma} \\ &= \frac{1}{\sigma} - \ln \Delta - \gamma + O(\sigma), \end{aligned} \quad (\text{B7})$$

where  $\sigma = 2 - d/2$ , and  $\gamma = 0.577\dots$  is the Euler–Mascheroni constant. For  $\sigma \neq 0$ , the limit  $\Lambda_o \rightarrow \infty$  may be taken since  $\sigma$  regulates the integral. For dressed particles,  $D_d$  must yield consistent results for both cutoff and dimensional regularization methods. Considering the requirements used to derive (B3) and employing appendix formulae in [22], we conclude

$$D_d = D(\Delta_o, \sigma). \quad (\text{B8})$$

For the processes in Fig. 3, the argument  $\Delta$  in (B7) has the form

$$\Delta(m, \mu) = am^2 + b\ell^2 + c\mu^2, \quad (\text{B9})$$

where  $m = m_b |m_f$ ,  $\ell^2 = k^2 | p^2 | q^2$ ,  $\{a, b, c\}$  depend on Feynman parameters, and  $c = 0$  for BSE processes. Applying (B4) to (B9) taking into account (15) and (16), the momenta go on-shell upon computing  $\lim_{\eta \rightarrow \infty} \eta_\lambda^{-2} \ell_d^2$ ; that is,

$$\begin{aligned} k^2 &\rightarrow m_b^2 && \text{BSE} \\ p^2 &\rightarrow m_f^2 && \text{FSE} \\ q^2 &\rightarrow 0 && \text{Vertex} \end{aligned}, \quad (\text{B10})$$

which we recognize as on-shell renormalization conditions. For the vertex, the dressed momentum transfer is

$$\begin{aligned} q_d &= q + \lambda(P'_M - P_M) \\ &= q, \end{aligned} \quad (\text{B11})$$

where  $P_M = M$  is the momentum of the self-mass; therefore,  $\lim_{\eta \rightarrow \infty} \eta_\lambda^{-2} q_d^2 = 0$ . The case where particle masses internal and external to the blob in Fig. 3 (a) are both zero occurs for BSE processes in the pure-gauge sector of QCD. For this case, where  $\Delta = bk^2$ , choose  $a = 1$  and introduce a small gluon mass  $m \rightarrow \mu_g$ , then using (D7), evaluate

$$\Delta_o = \lim_{\eta \rightarrow \infty} \eta_\lambda^{-2} \Delta(\eta_\lambda \mu_o) = \mu_o^2 \quad (\text{B12})$$

with  $\eta_\lambda = \sqrt{\lambda} \eta$ . Thus for all  $m \geq 0$ , the net S-matrix amplitude computed from (17) is well defined since it involves a factor

$$\frac{\Gamma(\sigma)}{\Delta^\sigma} - \frac{\Gamma(\sigma)}{\Delta_o^\sigma} = -\ln \left| \frac{\Delta}{\Delta_o} \right|. \quad (\text{B13})$$

The second term on the left side of (B13) is associated with an opposing vacuum energy required for overall energy conservation and system stability. In addition to a divergent part,  $\overline{\Omega}$  in (18) may include a finite part, a constant, that cancels a like term in  $\Omega$ .

### Appendix C: QED verification

Let us apply the foregoing theory with integration formulae given above to verify that net amplitudes for second order radiative corrections in Abelian QED are convergent and agree with results obtained via renormalization. Cutoff and dimensional regularization approaches are used to illustrate the method.

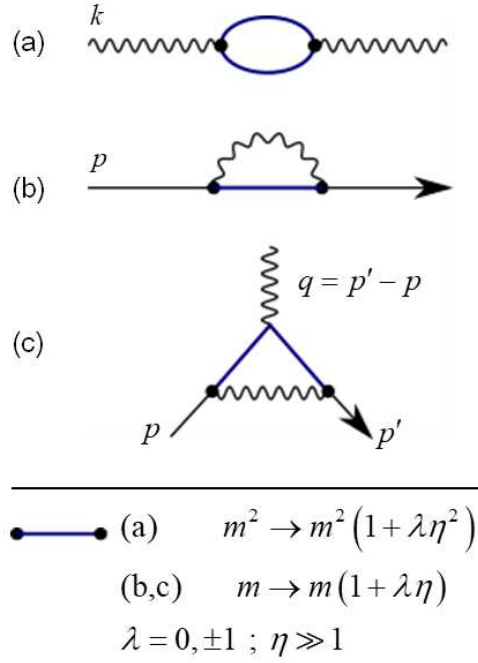


Figure 4. Baseline radiative corrections in QED: (a) photon self-energy, (b) fermion self-energy, and (c) vertex involve the core mass only in internal fermion lines. Two additional diagrams, obtained by replacing the core mass with electromagnetically dressed mass levels, are required for each radiative process to account for vacuum depletion and ensure stability.

### 1. Vacuum polarization

The photon self-energy associated with Fig. 4 (a) results in a propagator modification [9]

$$D_F^{\prime\alpha\beta} = D_F^{\alpha\beta} + D_F^{\alpha\mu} \left( i \hat{\Pi}_{\mu\nu} \right) D_F^{\nu\beta} ,$$

where

$$\hat{\Pi}_{\mu\nu} \equiv \Pi_{\mu\nu} - \bar{\Pi}_{\mu\nu}$$

is a polarization tensor generalized to include the stability correction, and

$$\Pi_{\mu\nu}(k, m) = -\frac{ie^2}{(2\pi)^4} \int d^4p \operatorname{tr} [\gamma_\mu S_F(p, m) \gamma_\nu S_F(p - k, m)]$$

follows from the Feynman-Dyson rules [8, 10]. In consequence of Lorentz and gauge invariance [42] or by direct calculation, it factors into

$$\Pi_{\mu\nu}(k, m) = \Pi(k^2, m^2) (g_{\mu\nu} k^2 - k_\mu k_\nu) .$$

As is well known, the contribution from terms  $k_\mu k_\nu$  vanishes due to current conservation upon connection to an external fermion line. For a massless photon,  $k^2$  is invariant under a DCM transform, and we need only focus on the scalar function  $\Pi(k^2, m^2)$ .

Since the scattering amplitude is in general a complex analytic function, it follows from Cauchy's formula that the real and imaginary parts are related by a dispersion relation [13]. The imaginary part is divergence free and may be obtained by replacing Feynman propagators with cut propagators on the mass shell according to Cutkosky's cutting rule [5] or, alternatively, via calculation in the Heisenberg representation as shown in Källén [25]. In particular for vacuum polarization, the real part is given by

$$\Pi(k^2, m^2) = \frac{1}{\pi} \int_{4m^2}^{4\Lambda_o^2} ds \frac{g\left(\frac{4m^2}{s}\right)}{s - k^2} \quad (C1)$$

with imaginary part

$$g(w) = -\frac{\alpha}{3}\sqrt{1-w}(1+w/2).$$

Applying (18) using (20) and (21) and performing a change of variables  $s = (1 + \lambda\eta^2)t$  in (C1), we have

$$\begin{aligned}\bar{\Pi} &= \frac{1}{2} \lim_{\eta \rightarrow \infty} \sum_{\lambda=\pm 1} \Pi(k^2, m^2 + \lambda\eta^2 m^2) \\ &= \frac{1}{2\pi} \lim_{\eta \rightarrow \infty} \sum_{\lambda=\pm 1} \int_{4m^2}^{4\Lambda_\circ^2} dt \frac{g\left(\frac{4m^2}{t}\right)}{t - (1 + \lambda\eta^2)^{-1} k^2}.\end{aligned}\tag{C2}$$

Letting  $\eta \rightarrow \infty$ , we see that (C2) is equivalent to a core amplitude evaluated on the light cone

$$\bar{\Pi} = \Pi(k^2 = 0, m^2).$$

Combining (C1) and (C2), we obtain a once-subtracted dispersion relation

$$\begin{aligned}\hat{\Pi}(k^2) &= \Pi(k^2, m^2) - \Pi(0, m^2) \\ &= \frac{k^2}{\pi} \int_{4m^2}^{\infty} ds \frac{g\left(\frac{4m^2}{s}\right)}{s(s-k^2)}\end{aligned}\tag{C3}$$

in agreement with renormalized QED. For massless photons,  $\hat{\Pi}(0) = 0$  represents a stability condition for vacuum polarization. For an infinite sum of 1PI insertions, the generalized photon propagator is

$$\begin{aligned}\text{Diagram with } k \text{ and a shaded circle} &= \text{Diagram with } k \text{ and a circle} + \text{Diagram with } k \text{ and two circles} + \dots \\ &= -\frac{ig_{\mu\nu}}{k^2} \hat{Z}_3(k^2),\end{aligned}\tag{C4}$$

where the finite stabilization parameter

$$\hat{Z}_3(k^2) = \frac{1}{1 - \hat{\Pi}(k^2)}\tag{C5}$$

modifies the free photon propagator. Alternatively, one can define a running coupling constant

$$\alpha(k^2) = \hat{Z}_3(k^2) \alpha_\circ;\tag{C6}$$

in this interpretation, the measured ( $\alpha_\circ = \frac{e^2}{4\pi}$ ) and effective couplings are equivalent on the light cone

$$\hat{Z}_3(0) = 1.\tag{C7}$$

Since a stationary state for a photon only exists on the light cone, the fundamental coupling is well defined there, and the stabilized photon self-energy vanishes.

In terms of an external current  $j_\mu^{ext}(x)$ , the observable current is given by

$$j_\mu^{obs}(x) = j_\mu^{ext}(x) + \delta j_\mu(x),$$

where

$$\delta j_\mu(x) = \frac{1}{(2\pi)^4} \int d^4k e^{ikx} j_\mu^{ext}(k) [\Pi(k^2) - \Pi(0)]$$

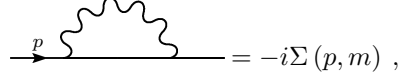
is the induced current. In standard renormalization theory (SRT), the last term in brackets is associated with a correction to a divergent bare charge ( $e_\circ$ ), but here, we assert that the correction is a stability requirement associated with opposing vacuum currents involving dressed fermions in the loop. Physical and bare charges in SRT are related by

$$e^2 = \left( Z_3 = \frac{1}{1 - \Pi(0, m^2)} \right) e_\circ^2,$$

where  $\sqrt{Z_3}$  is the charge renormalization constant. Charge renormalization in SRT is a consequence of neglecting vacuum depletion in violation of the law of conservation of energy.

## 2. Fermion self-energy

The fermion self-energy operator corresponding to the Feynman diagram in Fig. 4 (b) is



$$\text{Diagram} = -i\Sigma(p, m),$$

where

$$\Sigma(p, m) = -\frac{e^2}{(2\pi)^4} \int d^4k \gamma_\mu S_F(p-k, m) \gamma^\mu \frac{1}{k^2 - \mu^2}. \quad (\text{C8})$$

After standard reduction and dimensional regularization,  $\Sigma$  simplifies to

$$\Sigma(p, m) = \frac{\alpha}{2\pi} \left\{ S_1 + \int_0^1 dx [2m - \not{p}x + \sigma(\not{p}x - m)] D(\Delta, \sigma) \right\}, \quad (\text{C9})$$

where  $D(\Delta, \sigma)$  is given by (B7) with

$$\Delta = (1-x)(m^2 - xp^2) + x\mu^2.$$

The integral expression in (C9) is equivalent to a form given in [33], while the term

$$S_1 = -\frac{1-\sigma}{4} \not{p}$$

follows from appendix formulae in [24] and represents a surface contribution arising from a term linear in  $k$  during reduction of (C8).

Evaluation of  $\bar{\Sigma}$  using (18) reduces to negating (C9) and replacing  $\Delta \rightarrow \Delta_\circ$  according to (B8); we obtain

$$\bar{\Sigma}(p, m) = \frac{\alpha}{2\pi} \left\{ S_1 + \int_0^1 dx [2m - \not{p}x + \sigma(\not{p}x - m)] D(\Delta_\circ, \sigma) \right\}, \quad (\text{C10})$$

where

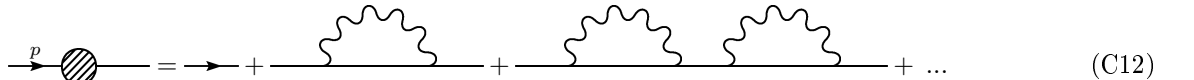
$$\Delta_\circ = m^2(1-x)^2 + x\mu^2$$

follows from (B10). Terms involving  $[(\lambda P_M, \lambda M); M = \eta m]$  have canceled in the average over DCM levels yielding a function of the observable mass and momentum only. The net correction, including all three mass levels in Fig. 4 (b), is given by (cf. [10])

$$\begin{aligned} \hat{\Sigma}(p) &= \Sigma - \bar{\Sigma} \\ &= \frac{\alpha}{2\pi} \int_0^1 dx (2m - \not{p}x) \ln \left[ \frac{m^2(1-x)^2 + x\mu^2}{(m^2 - xp^2)(1-x) + x\mu^2} \right], \end{aligned} \quad (\text{C11})$$

where the limit  $\sigma \rightarrow 0$  has been taken to recover four-dimensional spacetime. With a change of variables  $x = 1 - z$ , (C11) is seen to be identical to the renormalized result given in Bjorken & Drell [1].

The processes in Fig. 4 (b), including iterations in the series



$$\text{Diagram} = \text{Diagram} + \text{Diagram} + \text{Diagram} + \dots \quad (\text{C12})$$

yields a modified propagator [8, 9]

$$\begin{aligned} S'_F &= S_F + S_F \left( -i\hat{\Sigma}(p) \right) S'_F \\ &= \frac{i}{\not{p} - m - \hat{\Sigma}(p) + i\varepsilon}, \end{aligned} \quad (\text{C13})$$

which has the desired pole at  $\not{p} = m$  since (C11) vanishes on the mass shell

$$\hat{\Sigma}(\not{p})\Big|_{\not{p}^2=m^2} = 0. \quad (\text{C14})$$

Using the general expression for the stabilized fermion self-energy (E37)

$$\hat{\Sigma}(\not{p}) = \Sigma(\not{p}) - \Sigma(m) - \frac{\partial \Sigma}{\partial \not{p}}\Big|_{\not{p}=m}(\not{p} - m) \quad (\text{C15})$$

derived in Appendix E2, we see that

$$\frac{d\hat{\Sigma}(\not{p})}{d\not{p}}\Big|_{\not{p}=m} = 0,$$

and the residue of the propagator pole is  $i$ . For later use, we write (C13) in the form

$$\begin{array}{c} \rightarrow p \\ \text{---} \text{---} \text{---} \text{---} \text{---} \\ \text{---} \text{---} \text{---} \text{---} \text{---} \end{array} \text{---} \text{---} \text{---} \text{---} \text{---} = \frac{i}{\not{p} - m + i\varepsilon} \hat{Z}_2(\not{p}), \quad (\text{C16})$$

where

$$\hat{Z}_2 \equiv \left(1 - \frac{\hat{\Sigma}(\not{p})}{\not{p} - m + i\varepsilon}\right)^{-1} \quad (\text{C17})$$

is a finite stabilization parameter modifying the free field fermion propagator, and is analogous to the renormalization constant  $Z_2$  in SRT relating the bare and renormalized fields via  $\psi_o = \sqrt{Z_2}\psi$ .

Upon identifying

$$m_{em}^+ = \Sigma(\not{p} = m, \mu = 0) \quad \text{and} \quad (\text{C18})$$

$$m_{em}^- = -\overline{\Sigma}(\not{p} = m, \mu = 0), \quad (\text{C19})$$

we see that (C14) is equivalent to the FSE stability condition (3). Reverting to cutoff  $\Lambda_o$  using (B1), it follows that (C18) reduces to Feynman's result (2).

In the language of renormalization theory, the bare mass in the propagator [29]

$$S'_F = \frac{i}{\not{p} - m_{bare} - \Sigma + i\varepsilon}$$

must be renormalized using (6) with (C18); moreover, wave-field renormalization is required.

### 3. Vertex

A second-order correction to a corner (A15) involves a replacement

$$ie\gamma^\mu \rightarrow ie\Gamma^\mu,$$

where

$$\begin{aligned} \Gamma^\mu &= \gamma^\mu + \Lambda^\mu \\ &= \gamma^\mu F_1(q^2) + \frac{i\sigma^{\mu\nu}q_\nu}{2m} F_2(q^2), \end{aligned} \quad (\text{C20})$$

and  $\sigma^{\mu\nu} = \frac{i}{2} [\gamma^\mu, \gamma^\nu]$  are spin matrices. Complete expressions for the form factors  $F_1$  and  $F_2$  can be found in [33]. For small  $q^2$ , the vertex function  $\Lambda^\mu$  for  $\lambda = 0$  in Fig. 4 (c) is given by the approximation [10]

$$\Lambda^\mu(q, m) = \gamma^\mu L + a^{(2)} \frac{i\sigma^{\mu\nu} q_\nu}{2m} + O\left(\frac{q^2}{m^2}\right), \quad (\text{C21})$$

where

$$L = \frac{\alpha}{4\pi} \left( D_\circ + \frac{11}{2} - 4 \ln \frac{m}{\mu} \right) \quad (\text{C22})$$

is a divergent constant. Note that  $L = \frac{\alpha}{2\pi} r$ , where  $r$  is given by Eq. (23) in [10]. The coefficient  $a^{(2)} = \frac{\alpha}{2\pi}$  is the second-order contribution to the anomalous magnetic moment first derived by Schwinger [43] and verified experimentally by Foley & Kusch [12].

Inserting (C21) into (18), using

$$\mu \rightarrow \mu(1 + \lambda\eta), \quad (\text{C23})$$

and accounting for the invariance of  $D_\circ$  (B6) under scaling rules (20) and (21), the depletion correction is

$$\bar{\Lambda}^\mu = \gamma^\mu L,$$

where finite terms in (C21) of order  $O\left(\frac{q}{m}\right)$  involving replacements

$$m \rightarrow m(1 + \lambda\eta)$$

vanish in the limit  $\eta \rightarrow \infty$  as we argued in Appendix B. Therefore, the total vertex function

$$\hat{\Lambda}^\mu(q) = \Lambda^\mu - \bar{\Lambda}^\mu \quad (\text{C24})$$

is convergent, and  $\Lambda^\mu$  satisfies the usual renormalization condition for a vertex

$$\hat{\Lambda}^\mu \Big|_{q^2=0, \not{p}=\not{p}'=m} = 0. \quad (\text{C25})$$

This completes verification that lowest-order S-matrix corrections are finite without renormalization.

#### 4. Generalization to higher orders

Our next task is to show that stabilized higher-order radiative corrections in QED are finite and agree with renormalization. The proof closely follows arguments in references cited below and [24]; therefore, we keep our remarks brief highlighting required modifications and differences of interpretation.

Irreducible (skeleton) diagrams include second-order self-energy (SE) and vertex (V) parts discussed above plus infinitely many higher-order primitively divergent V-parts. Using Dyson's expansion method [9], second-order SE- and V-part operators for the core mass are

$$\Sigma = mA - (\not{p} - m)B + \hat{\Sigma}, \quad (\text{C26})$$

$$\Pi = C + \hat{\Pi}, \quad (\text{C27})$$

$$A^\mu = \gamma^\mu L + \hat{A}^\mu, \quad (\text{C28})$$

where  $\{A, B, C, L\}$  are logarithmically divergent coefficients depending on  $D_\circ$ . Higher-order primitively divergent V-parts are also of the form (C28) since the degree of divergence [9, 49]

$$K = 4 - \frac{3}{2}f_e - b_e$$

is zero (logarithmic), where  $f_e$  ( $b_e$ ) are the number of external fermion (boson) lines; in this case,  $L(D_\circ)$  is a power series in  $\alpha$ .

Applying (18) with (B6),

$$\bar{\Sigma} = mA - (\not{p} - m)B, \quad (\text{C29})$$

$$\bar{\Pi} = C, \quad (\text{C30})$$

$$\bar{A}^\mu = \gamma^\mu L, \quad (\text{C31})$$

where stabilized second-order amplitudes (C3), (C11), and (C24)

$$\hat{\Sigma}(p^2 = m^2) = 0, \quad (\text{C32})$$

$$\hat{\Pi}(k^2 = 0) = 0, \text{ and} \quad (\text{C33})$$

$$\hat{A}^\mu(q^2 = 0) = 0 \quad (\text{C34})$$

vanish on the mass shell. In renormalization theory, the term involving  $B$  in (C26) is eliminated by wave field renormalization. Higher-order primitively divergent V-parts also satisfy (C34) since dressed stabilized amplitudes vanish for on-shell conditions. In this way, (17) yields unique finite results

$$\hat{\Sigma} = \Sigma - \bar{\Sigma}, \quad (\text{C35})$$

$$\hat{\Pi} = \Pi - \bar{\Pi}, \text{ and} \quad (\text{C36})$$

$$\hat{A}^\mu = A^\mu - \bar{A}^\mu \quad (\text{C37})$$

for all irreducible diagrams; therefore, SE-part insertions

$$S_F \rightarrow S_F + S_F (-i\hat{\Sigma}) S_F \text{ and} \quad (\text{C38})$$

$$D_F^{\alpha\beta} \rightarrow D_F^{\alpha\beta} + D_F^{\alpha\mu} (ig_{\mu\nu} k^2 \hat{\Pi}) D_F^{\nu\beta} \quad (\text{C39})$$

into lines, and V-part insertions

$$\gamma^\mu \rightarrow \gamma^\mu + \hat{A}^\mu \quad (\text{C40})$$

into corners of a skeleton diagram yield no additional divergences.

For reducible vertex diagrams, the V-part resolves into a skeleton along with stabilized SE- and V-part insertions. With replacements (C38), (C39), and (C40) in the skeleton, the vertex operator again reduces to the form (C28), where  $L \rightarrow L_s$  is the skeleton divergence. In general,  $L_s$  depends on multiple functions  $D_\circ$  corresponding to all possible charged fermion masses arising from photon self-energy insertions which may in turn contain SE- and V-parts. Since each  $D_\circ$  is invariant under (B6), (C34) holds, and (18) yields

$$\bar{A}_s^\mu = \gamma^\mu L_s$$

similarly to (C31); therefore, the complete reducible V-part given by (C37) is convergent.

For reducible self-energy diagrams, a skeleton with SE insertions is handled in the same way as reducible vertex diagrams. However, vertex insertions into fermion and photon SE skeletons involve overlapping divergences that require further analysis [40, 48]. Integration of Ward's identities yields expressions of the same form as (C26) and (C27); in this case, the coefficients  $\{A, B, C\}$  are all power series in  $\alpha$  depending on  $D_\circ$ , and vertex insertions in SE-parts are convergent upon including stability corrections (C29) and (C30). We conclude that infinite field actions excite dressed mass levels uniformly in all connected fermion lines internal to overlapping loops; for a specific example, apply (17) to calculate the real part of the fourth-order vacuum polarization kernel [27] using the dispersion method given in Appendix C1. Therefore, a diagram with overlapping divergences is not a special case for implementation of stability corrections.

The complete propagators, replacing fermion and photon lines in a skeleton diagram, follow from Eqs. (63) and (64) of Dyson [9]; one obtains

$$S'_F(p) = \frac{i}{\not{p} - m - \hat{\Sigma}^* + i\varepsilon} \text{ and}$$

$$D'^{\alpha\beta}_F(k) = \frac{-ig^{\alpha\beta}}{k^2 [1 - \hat{\Pi}^*] + i\varepsilon},$$

where  $\{\hat{\Sigma}^*, \hat{\Pi}^*\}$  are given by sums over all proper SE-parts. Similarly, the most general vertex replacing a corner in a skeleton diagram is given by a sum over all proper V-parts. Since both core and stability corrections are included in each sub-diagram, the complete propagators and vertices are well defined (convergent).



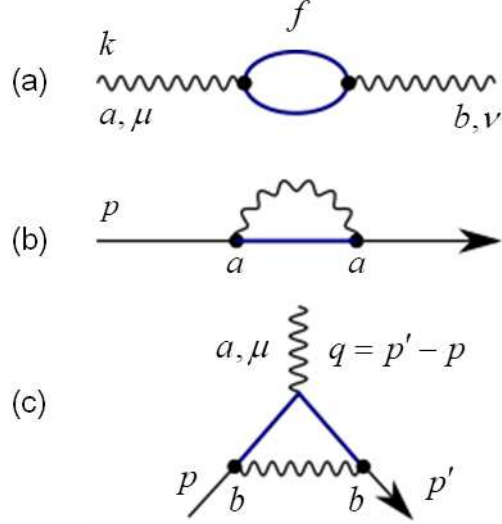


Figure 5. Gluon/quark self-energies and vertex diagrams

#### Appendix D: QCD verification

In the examples below, we focus on a key subset of one-loop diagrams [15, 36] that occur in the  $SU(3)$  Yang-Mills theory; see Appendix A 2 for nomenclature.

For diagrams in Fig. 5, core amplitudes differ from QED only by group factors and switching factor  $\lambda_s$  from (23); therefore, finite S-matrix amplitudes (22), including stability corrections, are

$$\hat{\Pi}_1^{ab} = \lambda_s \text{tr}(t^a t^b) \hat{\Pi}[QED], \quad (D1)$$

$$\hat{\Sigma}^{aa} = \lambda_s t^a t^a \hat{\Sigma}[QED], \quad \text{and} \quad (D2)$$

$$\hat{\Lambda}_1^{a,\mu} = \lambda_s t^b t^a t^b \hat{\Lambda}^\mu[QED]. \quad (D3)$$

Group factors are given by

$$\begin{aligned} \text{tr}(t^a t^b) &= C(r) \delta^{ab}, \\ t^a t^a &= C_2(r), \\ t^b t^a t^b &= \left[ C_2(r) - \frac{1}{2} C_2(G) \right] t^a, \end{aligned}$$

where  $C(N) = \frac{1}{2}$  and  $C_2(N) = \frac{N^2-1}{2N} = \frac{4}{3}$  are normalization and quark color charge factors, respectively.

In addition to the fermion (quark) loop diagram in Fig. 5 (a), gluon self-energy corrections in Fig. 6 yield [33]

$$[\text{Fig. 6}] = iT_{\mu\nu}(k^2) \delta^{ab} \Pi_2(k^2), \quad (D4)$$

$$T_{\mu\nu}(k^2) = g_{\mu\nu} k^2 - k_\mu k_\nu,$$

$$\Pi_2(k^2) = \frac{\alpha_s C_2(G)}{4\pi} \int_0^1 dx \frac{\Gamma(\sigma)}{\Delta^\sigma} \left[ (\sigma-1)(1-2x)^2 + 2 \right], \quad (D5)$$

where  $\alpha_s = g_s^2/4\pi$  is the strong coupling constant,  $\Delta = -k^2 x(1-x)$ , and  $x$  is a Feynman parameter. While individual gluons are massless to ensure gauge invariance of  $\mathcal{L}_{YM}$ , systems of gluons depicted in Fig. 6 are expected to have a non-zero mass defined by (7) with self-energy function

$$\Sigma^g \sim k^2 \Pi_2. \quad (D6)$$

The generation of such systems redistributes vacuum energy as indicated in Fig. 1. Consequently, we need to include a stability correction involving DCM states, but for this we need a mass term in  $\Delta$ . If we appeal to massive Yang-Mills theories [20], we get unwanted particles and ghosts, and it might seem that we have an impasse. While gauge invariance demands that mass be acquired via a Higgs mechanism, introduction of dressed masses in (A22) yielding

$$\mathcal{L}'_{YM} \rightarrow \mathcal{L}_{YM} - \frac{1}{2} \sum_{\lambda=\pm 1} [\mu_g^2 + \lambda M_g^2]_{\mu_g=0} (A_\mu^a)^2$$

does not break gauge invariance of  $\mathcal{L}_{YM}$  since its sum is zero. Therefore, let us temporarily assign a small mass  $\mu_g$  to the gluon, then propagators in the loops are modified

$$\frac{1}{p^2 - \mu_g^2} \frac{1}{(p+k)^2 - \mu_g^2} = \int_0^1 \frac{dx}{[P^2 - \Delta(\mu_g)]^2},$$

where the usual change of variables  $P = p + xk$  has been made for loop integration parameter  $p$ , and

$$\Delta(\mu_g) = \mu_g^2 - k^2 x(1-x).$$

To evaluate the stability contribution, let  $M_g = \eta\mu_o$ , where  $\mu_o$  is an arbitrary unit of mass measure. Substituting

$$\mu_g^2 \rightarrow [\mu_g^2 + \lambda\eta^2\mu_o^2]_{\mu_g=0} \quad (\text{D7})$$

in  $\Delta(\mu_g)$  and using (B12), we have  $\Delta_o = \mu_o^2$ . Negating (D5), replacing

$$\frac{1}{\Delta^\sigma} \rightarrow \frac{1}{\Delta_o^\sigma},$$

and using (22), the net amplitude

$$\hat{\Pi}_2(k^2) = -\lambda_s \frac{\alpha_s C_2(G)}{4\pi} \int_0^1 dx \ln \left[ \frac{-k^2 x(1-x)}{\mu_o^2} \right] [2 - (1-2x)^2] \quad (\text{D8})$$

is finite. If we define a reference mass  $M_s$  by

$$\frac{5}{3} \ln \left( \frac{\mu_o^2}{M_s^2} \right) \equiv \int_0^1 dx \ln [x(1-x)] [2 - (1-2x)^2],$$

then

$$\hat{\Pi}_2 \left( \rho_s \equiv -\frac{k^2}{M_s^2} \right) = -\lambda_s \frac{\alpha_s C_2(G)}{4\pi} \frac{5}{3} \ln \rho_s \quad (\text{D9})$$

vanishes at spacelike  $k^2 = -M_s^2$ . For physically meaningful interpretation of the amplitudes, unobservable quark and gluon states must have negative norm and spacelike momenta.

In the stabilized theory, it is invalid to neglect quark masses  $m_f$  in the calculations since they are required for defining dressed amplitudes, but QCD calculations in the usual theory often omit  $m_f$  in processes where the momentum transfer  $q$  is presumed much larger than physical masses involved in the problem. Therefore, following Peskin & Schroeder [33], but assuming  $m \equiv m_f \neq 0$ , the stabilized integral for the quark/three-gluon vertex shown in Fig. 7 is

$$\hat{A}_2^{a,\mu} = i\lambda_s \frac{g_s^2 C_2(G) t^a}{(2\pi)^4} \int dx dy dz \delta(x+y+z-1) \Delta I^\mu, \quad (\text{D10})$$

where  $(x, y, z)$  are Feynman parameters; keeping only leading logarithmic terms,

$$\begin{aligned} \Delta I^\mu &\simeq I^\mu - \bar{I}^\mu \\ &= 3i\pi^2 \gamma^\mu \ln \frac{\Delta}{\Delta_o}, \end{aligned}$$

$$I^\mu = -3i\pi^2 \gamma^\mu \frac{\Gamma(\sigma)}{\Delta^\sigma},$$

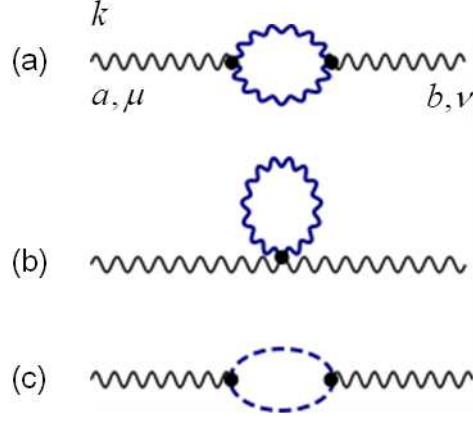


Figure 6. Gluon self-energy corrections in pure-gauge sector: (a) gluon loop, (b) four-gluon vertex, and (c) ghost loop.

$$\Delta = m^2 z + (px + p'y)^2 - p^2 x - p'^2 y + \mu^2 (1 - z) ,$$

$$\bar{I}^\mu = -3i\pi^2 \gamma^\mu \frac{\Gamma(\sigma)}{\Delta_\circ^\sigma} ,$$

and

$$\Delta_\circ = m^2 z^2 + \mu^2 (1 - z)$$

using (B4). Assuming  $p$  is on mass shell and  $-q^2 \gg m^2 \gg \mu^2$ ,  $\Delta \simeq -q^2 y (1 - y)$  and  $\Delta_\circ \simeq m^2 z^2$ ; therefore,

$$\Delta I^\mu \simeq 3i\pi^2 \gamma^\mu \ln \frac{-q^2}{m^2} + \text{H.O.T.} .$$

Higher order terms in  $\Delta I^\mu$  integrate to  $O(1)$  in (D10), and we have

$$\hat{\Lambda}_2^{a,\mu} = -\lambda_s \frac{\alpha_s}{4\pi} \frac{3}{2} C_2(G) t^a \gamma^\mu \ln \frac{-q^2}{m^2} . \quad (\text{D11})$$

It remains to show that the stabilized theory agrees with standard renormalization theory and experimental data [7]; in particular, an effective weakening of the strong coupling for high energies consistent with asymptotic freedom predictions [16, 35]. Well known formulae from SRT are used, where renormalization constants are replaced with stabilized amplitude parameters

$$Z_i \rightarrow \hat{Z}_i , \quad i = 1, 2, 3 .$$

Leading terms of stabilized amplitudes for the asymptotic case of high energy yield an effective color charge

$$\begin{aligned} \bar{g}_s(\rho_s) &= g_s \frac{\hat{Z}_1}{\hat{Z}_2 \sqrt{\hat{Z}_3}} \\ &\simeq g_s \left[ 1 + \lambda_s \frac{\alpha_s}{8\pi} \left( 11 - \frac{2}{3} n_f \right) \ln \rho_s \right] , \end{aligned} \quad (\text{D12})$$

where

$$\hat{Z}_1^{-1} = 1 + \hat{\Lambda}_1(\rho_s) + \hat{\Lambda}_2(\rho_s) , \quad (\text{D13})$$

$$\hat{Z}_2^{-1} = 1 - \left. \frac{d\hat{\Sigma}}{d\phi} \right|_{\rho=\rho_s} , \quad \text{and} \quad (\text{D14})$$

$$\hat{Z}_3^{-1} = 1 - \left[ \hat{\Pi}_1(\rho_s) + \hat{\Pi}_2(\rho_s) \right] \quad (\text{D15})$$

are finite running stabilization parameters that modify the vertex (A23), fermion field propagator (A18), and gluon field propagator (A24), respectively. For loops including quarks, asymptotic amplitudes involve spacelike momenta  $\ell$  in quadratic energy ratios

$$\rho = -\frac{\ell^2}{m_f^2} \gg 1; \ell^2 \in \{k^2, p^2, q^2\}, \quad (\text{D16})$$

where we have reinstated  $m_f = m$ . Setting  $p^2 = q^2 = k^2$  across diagrams and neglecting  $O(1)$  terms in

$$\begin{aligned} \ln \rho &= \ln \rho_s + O(1) \\ &\simeq \ln \rho_s, \end{aligned} \quad (\text{D17})$$

where  $\rho_s = -k^2/M_s^2$ , the sum over fermions in Fig. 5(a) becomes trivial, and we have

$$\sum_{f=1}^{n_f} \left\{ [\text{Fig. 5(a)}] = \text{diagram} \right\} \simeq iT_{\mu\nu}(k^2) \delta^{ab} \left[ \hat{\Pi}_1(\rho_s) \equiv \lambda_s \frac{\alpha_s}{3\pi} n_f C(r) \ln \rho_s \right], \quad (\text{D18})$$

$$[\text{Fig. 5(b)}] \simeq -i \left[ \hat{\Sigma}(\not{p}, \rho_s) \equiv \lambda_s \frac{\alpha_s}{4\pi} C_2(r) (\not{p} - 4m_f) \ln \rho_s \right], \quad (\text{D19})$$

$$[\text{Fig. 5(c)}] \simeq ig_s t^a \gamma^\mu \left\{ \hat{A}_1(\rho_s) \equiv -\lambda_s \frac{\alpha_s}{4\pi} \left[ C_2(r) - \frac{1}{2} C_2(G) \right] \ln \rho_s \right\}, \quad (\text{D20})$$

$$[\text{Fig. 6}] = iT_{\mu\nu}(k^2) \delta^{ab} \left[ \hat{\Pi}_2(\rho_s) \equiv -\lambda_s \frac{\alpha_s C_2(G)}{4\pi} \frac{5}{3} \ln \rho_s \right], \text{ and} \quad (\text{D21})$$

$$[\text{Fig. 7}] \simeq ig_s t^a \gamma^\mu \left[ \hat{A}_2(\rho_s) \equiv -\lambda_s \frac{\alpha_s}{4\pi} \frac{3}{2} C_2(G) \ln \rho_s \right]. \quad (\text{D22})$$

With the approximation  $-k^2 \gg m_f^2$ ,  $\hat{\Pi}_1$  in (D18) follows from (D1) using (C3). Similarly,  $\hat{\Sigma}$  in (D19) is obtained from (D2) using (C11), and  $\hat{A}_1$  in (D20) is derived using (D3) with (C20). The stabilization parameters  $\hat{Z}_1$ ,  $\hat{Z}_2$ , and  $\hat{Z}_3$  are defined similarly to their SRT counterparts.  $\hat{Z}_1^{-1}$  is the coefficient of  $ig_s \gamma^\mu t^a$  for the sum of proper vertex diagrams in (A23), Fig. 5(c), and Fig. 7:

$$\text{diagram} \cdot (1 + \hat{A}_1 + \hat{A}_2) \equiv ig_s \gamma^\mu t^a \hat{Z}_1^{-1}.$$

Using (C17) or (D14) and assuming  $-p^2 \gg m_f^2$ , we have

$$\hat{Z}_2^{-1} = 1 - \lambda_s \frac{\alpha_s}{4\pi} C_2(r) [\ln \rho = \ln \rho_s + O(1)].$$

For  $\hat{Z}_3$ , (C5) is used with  $\hat{H} = \hat{\Pi}_1 + \hat{\Pi}_2$ , (D18), and (D21).

Finally, using (D12), the effective coupling constant is reduces to

$$\bar{\alpha}_s(\rho_s) = \frac{\alpha_s}{1 - \lambda_s \frac{\alpha_s}{4\pi} \left( 11 - \frac{2}{3} n_f \right) \ln \rho_s + O(\ln^2 \rho_s)}. \quad (\text{D23})$$

Neglecting terms of  $O(\ln^2 \rho_s)$  for  $\rho_s$  near one and requiring  $\lambda_s = -1$ , (D23) reduces to the expected result for asymptotic freedom. The corresponding Callan-Symanzik [3, 46] beta function is

$$\beta_{QCD} = 2 \frac{\partial \bar{\alpha}_s}{\partial \ln \rho_s} \Big|_{\rho_s=1} = \lambda_s \frac{\alpha_s^2}{2\pi} \left( 11 - \frac{2}{3} n_f \right). \quad (\text{D24})$$

The foregoing results are consistent with Fig. 1 and in complete agreement with standard QFT. The effective color charge in (D12) is defined relative to a stable value  $g_s$  defined at the near-field boundary, where the gluon polarization function (D9) vanishes at  $-k^2 = M_s^2$ , and  $\Sigma^g$  in (D6) goes positive for  $-k^2 > M_s^2$ . In contrast to this, low energy electron scattering processes probe the far-field (positive energy) region, and a stable value for the electric charge is defined in the free particle limit:  $k^2 = 0$ , where the polarization function  $\hat{\Pi}(k^2)$  vanishes; refer to Eqs. (C3)-(C7).

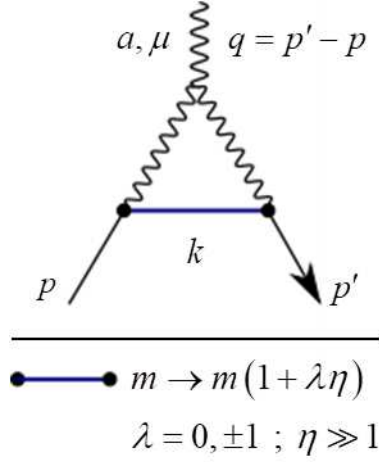


Figure 7. Quark/three-gluon vertex.

An estimate of  $M_s$  may be obtained by synchronizing  $\rho$  in (D16) across diagrams in Fig. 5 (a) with that for  $\rho_s$  in (D9) for Fig. 6: Let  $k \rightarrow \ell$  in Fig. 5 (a), and require

$$\frac{\ell^2}{m_f^2} = \frac{k^2}{M_s^2}. \quad (\text{D25})$$

Noting that  $\hat{\Pi}[QED]$  is a function of  $\rho$  only from (C3) and using (D25), the sum over fermions is given by

$$\sum_{f=1}^{n_f} \text{diagram}(\ell, a, \mu, f, b, \nu) = \left[ \left( \frac{1}{n_f} \sum_{f=1}^{n_f} \frac{m_f^2}{M_s^2} \right) \equiv 1 \right] n_f \text{diagram}(k, a, \mu, f, b, \nu). \quad (\text{D26})$$

The condition in brackets is obtained by factoring

$$T_{\mu\nu}(\ell^2) = \frac{m_f^2}{M_s^2} T_{\mu\nu}(k^2)$$

and comparing with (D18), then we have

$$M_s^2 = \frac{1}{n_f} \sum_{f=1}^{n_f} m_f^2 \quad (\text{D27})$$

for the reference mass. Evaluating (D27) for quarks gives  $M_s = 70.65 \text{ GeV}/c^2$ ; compare with Z-boson mass given in Appendix F: Table II.

### Appendix E: Electroweak verification

We compute finite electroweak amplitudes using dimensionally regularized radiative corrections for unrenormalized (core) functions [2, 19, 32]. One-loop self-energy functions include  $\Sigma^{ab}$  for bosons, where

$$ab \in \{\gamma\gamma, \gamma Z, ZZ, WW\}$$

defines particles external to the loop,  $\Sigma^f$  for fermions ( $f = j\sigma$  for family  $j$  and doublet index  $\sigma = \pm$ ), and vertex  $A_\mu^{\gamma f}$ . For repeated indices  $a = b$ , we abbreviate  $\Sigma^b \equiv \Sigma^{bb}$  with  $b \in \{\gamma, Z, W\}$ ; in general formulae applicable to  $\gamma - Z$  mixing, we admit  $b = \gamma Z$  as well for brevity. A subscript “sa” is appended to a stabilized amplitude  $\hat{\Sigma}^b \equiv \hat{\Sigma}_{sa}^b$  when it is necessary to distinguish it from a corresponding renormalized amplitude  $\hat{\Sigma}_{ra}^b$ .

In Hollik’s notation [19], the basic singular function

$$\Delta_\kappa = \frac{1}{\sigma} - \gamma - \ln \frac{m_\kappa^2}{\mu_0^2} + \ln 4\pi \quad (\text{E1})$$

differs from (B7) by finite terms. For consistency, the input momentum to a loop is  $k$  with  $s \equiv k^2$  for both bosons and fermions. Abbreviations for squared boson masses

$$z = m_Z^2, \quad w = m_W^2, \quad \text{and} \quad h = m_H^2$$

are used. In addition to (E1), core amplitudes involve finite functions

$$\bar{B}_o(s, m_1, m_2) = - \int_0^1 dx \ln \left[ \frac{x^2 s - x(s + m_1^2 - m_2^2) + m_1^2 - i\epsilon}{m_1 m_2} \right], \quad (\text{E2})$$

$$F(s, m_1, m_2) = -1 + \frac{m_1^2 + m_2^2}{m_1^2 - m_2^2} \ln \frac{m_1}{m_2} + \bar{B}_o(s, m_1, m_2), \quad (\text{E3})$$

$$\bar{B}_1(s, m_1, m_2) = -\frac{1}{4} + \frac{m_1^2}{m_1^2 - m_2^2} \ln \frac{m_1}{m_2} + \frac{m_2^2 - m_1^2 - s}{2s} F(s, m_1, m_2), \quad (\text{E4})$$

and singular expressions

$$B_o(s, m_1, m_2) = \frac{1}{2} (\Delta_{m_1} + \Delta_{m_2}) + \bar{B}_o(s, m_1, m_2) \quad \text{and} \quad (\text{E5})$$

$$B_1(s, m_1, m_2) = -\frac{1}{2} \left( \Delta_{m_2} + \frac{1}{2} \right) + \bar{B}_1(s, m_1, m_2). \quad (\text{E6})$$

Scalar one-loop integrals, including (E2), are defined in [23].

### 1. Boson self-energy corrections

For these corrections, it is useful to expand the boson self-energy

$$\Sigma^b(s) = \Sigma^b(m_b^2) + \sum_{n=1}^{\infty} \frac{\partial^n \Sigma^b}{\partial s^n} \Big|_{s=m_b^2} (s - m_b^2)^n. \quad (\text{E7})$$

From core amplitudes, it can be seen by inspection and dimensional analysis that averages of  $\Sigma^b(m_b^2)$  and  $\frac{\partial \Sigma^b}{\partial s} \Big|_{s=m_b^2}$  over DCM levels in (18) are stationary. For mass set

$$\{m_\kappa\} \subseteq \{m_f, m_W, m_Z, m_H\},$$

the DCM transform (13) is

$$\{m_\kappa^2\} \rightarrow \{m_\kappa^2\} \cdot (1 + \lambda\eta^2). \quad (\text{E8})$$

On the mass shell, the self-energy function has the general form

$$\Sigma^b(m_b^2) = \sum_{\kappa} \alpha_\kappa^b m_\kappa^2,$$

where  $\alpha_\kappa^b$  are dimensionless coefficients which may depend on invariant mass ratios. Therefore, under (E8)

$$\Sigma^b(m_b^2) \rightarrow (1 + \lambda\eta^2) \Sigma^b(m_b^2),$$

and the average

$$\begin{aligned} \bar{\Sigma}^b(m_b^2) &= \frac{1}{2} \sum_{\lambda=\pm 1} (1 + \lambda\eta^2) \Sigma^b(m_b^2) \\ &= \Sigma^b(m_b^2) \end{aligned} \quad (\text{E9})$$

over dressed states is stationary. Since the derivative  $\left. \frac{\partial \Sigma^b}{\partial s} \right|_{s=m_b^2}$  is dimensionless, it is invariant under (E8). Finally, higher order derivatives are either zero outright, or

$$\left. \frac{\partial^n \Sigma^b}{\partial s^n} \right|_{s=m_b^2} \sim (m_b^2)^{1-n} \rightarrow O\left(\eta^{2(1-n)}\right) \quad (\text{E10})$$

vanishes under (E8) as  $\eta \rightarrow \infty$  for  $n \geq 2$ . Therefore, (18) yields

$$\overline{\Sigma}^b(s) = \Sigma^b(m_b^2) + \left. \frac{\partial \Sigma^b}{\partial s} \right|_{s=m_b^2} (s - m_b^2) . \quad (\text{E11})$$

Since the off-shell factor  $s - m_b^2 = \delta k_{\partial s}^2$  is invariant under (E8), the entire expression (E11) is stationary under an average over DCM levels similarly to (E9). The net stabilized amplitude

$$\hat{\Sigma}^b(s) = \Sigma^b(s) - \overline{\Sigma}^b(s) \quad (\text{E12})$$

from (17) satisfies stability conditions

$$\hat{\Sigma}^b(m_b^2) = 0 \text{ and} \quad (\text{E13})$$

$$\left. \frac{\partial \hat{\Sigma}^b(s)}{\partial s} \right|_{s=m_b^2} = 0 . \quad (\text{E14})$$

Taking the real part of (E13) and (E14) yields renormalization conditions [6], which differ from those given in [19]. For stabilized amplitude (E12), (E13) and (E14) yield a propagator residue of unity so there is no need for external wave function corrections as in the on-shell renormalization scheme proposed by Ross and Taylor [39]; however, inclusion of  $\Delta r$  corrections [44] discussed in Appendix E 4 leads to finite wave field corrections. Splitting off singular terms (E1), the boson self-energy can be expressed in the form

$$\Sigma^b(s) = \sum_{\kappa} [\alpha_{\kappa}^b s \Delta_{\kappa} + \beta_{\kappa}^b m_{\kappa}^2 \Delta_{\kappa}] + \Sigma_{finite}^b(s) , \quad (\text{E15})$$

where  $\{\alpha_{\kappa}^b, \beta_{\kappa}^b\}$  are constant coefficients. Singular terms involving  $\{s \Delta_{\kappa}, m_{\kappa}^2 \Delta_{\kappa}\}$  in  $\overline{\Sigma}^b$  cancel those in  $\Sigma^b$ , and (E12) reduces to

$$\hat{\Sigma}^b(s) = \Sigma_{finite}^b(s) - \Sigma_{finite}^b(m_b^2) - \left. \frac{\partial \Sigma_{finite}^b}{\partial s} \right|_{s=m_b^2} (s - m_b^2) . \quad (\text{E16})$$

For a free boson, the squared mass shift

$$\delta m_b^2 \equiv \text{Re} [\Sigma_{finite}^b(m_b^2)] \quad (\text{E17})$$

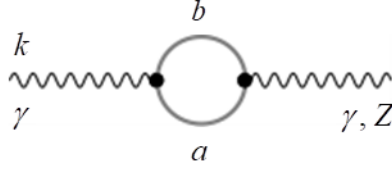
represents the residual boson self-energy of the core after divergent parts of  $\overline{\Sigma}^b(m_b^2)$  have canceled those in (E15). For later reference, the polarization function is

$$\hat{H}^b(s) = \frac{\hat{\Sigma}^b(s)}{s - m_b^2} = \frac{\Sigma^b(s) - \Sigma^b(m_b^2)}{s - m_b^2} - \left. \frac{\partial \Sigma^b}{\partial s} \right|_{s=m_b^2} . \quad (\text{E18})$$

Neglecting  $\Delta r$  corrections, mixing angle functions  $c_w = \cos \theta_W$  (A5) and  $s_w = \sin \theta_W$ , and neutral current constants (A17) are invariant under (E8). See (E28) and (E29) for inclusion of  $\Delta r$ .

Application of (E12) to photon self-energy corrections shown in Fig. 8 yields

$$\begin{aligned} \hat{\Sigma}^{\gamma}(s) &= \Sigma^{\gamma}(s) - \overline{\Sigma}^{\gamma}(s) \\ &= \frac{\alpha}{4\pi} \left\{ \frac{4}{3} \sum_f Q_f^2 \left[ (s + 2m_f^2) F(s, m_f, m_f) - \frac{s}{3} \right] \right. \\ &\quad \left. - (3s + 4w) F(s, m_W, m_W) + \frac{2}{3}s \right\} , \end{aligned} \quad (\text{E19})$$



$a$	$b$
$\bar{f}$	$f$
$W$	$W$
$\phi$	$W$
$\phi$	$\phi$
$u^\pm$	$u^\pm$
$\dagger$	$W, \phi$

† Four gauge boson vertex with internal  $W, \phi$

Figure 8. Photon self-energy and photon-Z mixing diagrams.

$$\Sigma^\gamma(s) = \frac{\alpha}{4\pi} \left\{ \frac{4}{3} \sum_f Q_f^2 \left[ s\Delta_f + (s + 2m_f^2) F(s, m_f, m_f) - \frac{s}{3} \right] - 3s\Delta_W - (3s + 4w) F(s, m_W, m_W) \right\}, \quad (\text{E20})$$

$$\bar{\Sigma}^\gamma(s) = \Sigma^\gamma(0) + \left. \frac{\partial \Sigma^\gamma}{\partial s} \right|_{s=0} s, \quad (\text{E21})$$

where

$$\Sigma^\gamma(0) = 0, \quad \left. \frac{\partial \Sigma^\gamma}{\partial s} \right|_{s=0} = \frac{\alpha}{4\pi} \left\{ \frac{4}{3} \sum_f Q_f^2 \Delta_f - 3\Delta_W - \frac{2}{3} \right\},$$

and the sum over fermions includes color for the case of quarks. Both  $\hat{\Sigma}^\gamma(s)$  and  $\hat{\Pi}^\gamma(s)$  vanish in the Thomson limit  $s \rightarrow 0$ , and physically meaningful corrections in (E19) are due to incomplete cancellation for  $s = k^2 \neq 0$ . Singular terms in  $\bar{\Sigma}^\gamma$  exactly cancel those in  $\Sigma^\gamma$  for all  $s$ , and there remains a term

$$\left[ \bar{\Sigma}^\gamma \right]_{finite} = - \left( \delta\alpha_{finite} \equiv \frac{\alpha}{6\pi} \right) s \quad (\text{E22})$$

in the vacuum response, where  $\delta\alpha_{finite}$  is the finite part of renormalization constant  $\delta Z_2^\gamma$  in the usual theory.

For  $\gamma - Z$  mixing corrections also represented in Fig. 8, we have

$$\begin{aligned} \hat{\Sigma}^{\gamma Z}(s) &= \Sigma^{\gamma Z} - \bar{\Sigma}^{\gamma Z} \\ &= \frac{\alpha}{4\pi} \left\{ -\frac{4}{3} \sum_f Q_f v_f \left[ (s + 2m_f^2) F(s, m_f, m_f) - \frac{s}{3} \right] \right. \\ &\quad \left. + \frac{1}{c_w s_w} \left[ \left( 3c_w^2 + \frac{1}{6} \right) s + \left( 4c_w^2 + \frac{4}{3} \right) w \right] F(s, m_W, m_W) - \frac{s}{6c_w s_w} \left( 4c_w^2 + \frac{4}{3} \right) \right\}, \end{aligned} \quad (\text{E23})$$



$$\begin{aligned} \Sigma^{\gamma Z}(s) = & \frac{\alpha}{4\pi} \left\{ -\frac{4}{3} \sum_f Q_f v_f \left[ s \Delta_f + (s + 2m_f^2) F(s, m_f, m_f) - \frac{s}{3} \right] \right. \\ & + \frac{1}{c_w s_w} \left[ \left( 3c_w^2 + \frac{1}{6} \right) s + 2w \right] \Delta_W \\ & \left. + \frac{1}{c_w s_w} \left[ \left( 3c_w^2 + \frac{1}{6} \right) s + \left( 4c_w^2 + \frac{4}{3} \right) w \right] F(s, m_W, m_W) + \frac{s}{9c_w s_w} \right\}, \end{aligned} \quad (\text{E24})$$

$$\bar{\Sigma}^{\gamma Z} = \Sigma^{\gamma Z}(0) + \left. \frac{\partial \Sigma^{\gamma Z}}{\partial s} \right|_{s=0} s, \quad (\text{E25})$$

where

$$\begin{aligned} \Sigma^{\gamma Z}(0) &= \frac{\alpha}{4\pi} \left\{ \frac{2w}{c_w s_w} \Delta_W \right\}, \\ \left. \frac{\partial \Sigma^{\gamma Z}}{\partial s} \right|_{s=0} &= \frac{\alpha}{4\pi} \left\{ -\frac{4}{3} \sum_f Q_f v_f \Delta_f + \frac{1}{c_w s_w} \left[ \left( 3c_w^2 + \frac{1}{6} \right) \Delta_W + \frac{1}{6} \left( 4c_w^2 + \frac{4}{3} \right) + \frac{1}{9} \right] \right\}, \end{aligned}$$

and  $\Sigma^{\gamma Z}(0) \neq 0$  is due to non-Abelian boson loops in Fig. 8.

Renormalization starts with a bare charge  $e_o$ , and the correction [2]

$$\begin{aligned} \delta e(\Pi^\gamma, \Sigma^{\gamma Z}) &= e_o \left[ \delta Z_1^\gamma - \frac{3}{2} \delta Z_2^\gamma \right] \\ &= e_o \left[ \frac{1}{2} \Pi^\gamma(0) - \frac{s_w}{c_w} \frac{\Sigma^{\gamma Z}(0)}{m_Z^2} \right] \end{aligned} \quad (\text{E26})$$

renormalizes the charge  $e = e_o + \delta e$ , where

$$\begin{aligned} \delta Z_1^\gamma &= -\Pi^\gamma(0) - \frac{s_w}{c_w} \frac{\Sigma^{\gamma Z}(0)}{m_Z^2} \quad \text{and} \\ \delta Z_2^\gamma &= -\Pi^\gamma(0) \end{aligned}$$

are the charge and photon field renormalization constants, respectively. In the usual theory, arguments on the left in (E26) are core functions  $\{\Pi^\gamma, \Sigma^{\gamma Z}\}$ ; however, in the stabilized theory, we utilize the complete amplitudes (E19) and (E23) to obtain

$$\delta e(\hat{\Pi}^\gamma, \hat{\Sigma}^{\gamma Z}) = 0. \quad (\text{E27})$$

Therefore,  $e = e_o$ , and there is no charge renormalization.

Self-energy diagrams for the  $Z$ - and  $W$ -bosons are tabulated in Figs. 9 and 10, respectively. Due to their complexity, analytic expressions for the unrenormalized amplitudes [19] are omitted here, but the stabilized amplitudes are easily evaluated using (E11) and analytic expressions for partials  $\frac{\partial \Sigma^b}{\partial s}$ . Plots of these functions are given in Appendix F.

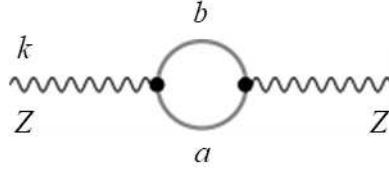
Self-energies for diagrams with  $b \in \{\gamma Z, Z, W\}$  require adjustments

$$\hat{\Sigma}^b(s) \rightarrow \hat{\Sigma}^b(s) + (s - m_b^2) \Delta r^b \quad (b = W, Z) \quad \text{and} \quad (\text{E28})$$

$$\hat{\Sigma}^{\gamma Z}(s) \rightarrow \hat{\Sigma}^{\gamma Z}(s) + s \Delta r^{\gamma Z} \quad (\text{E29})$$

for  $\Delta r$  corrections [44] which account for variations of  $\{g_W, g_Z\}$  with respect to  $m_W$  and  $m_Z$ ; we have

$$\{\Delta r^{\gamma Z}, \Delta r^Z, \Delta r^W\} = \left\{ -\frac{c_w}{s_w}, \frac{c_w^2 - s_w^2}{s_w^2}, \frac{c_w^2}{s_w^2} \right\} \left( \frac{\delta m_Z^2}{m_Z^2} - \frac{\delta m_W^2}{m_W^2} \right), \quad (\text{E30})$$



$a$	$b$
$\bar{f}$	$f$
$W$	$W$
$\phi$	$W$
$H$	$Z$
$\chi$	$H$
$\phi$	$\phi$
$u^\pm$	$u^\pm$
$\dagger$	$W, H, \chi, \phi$

Figure 9. Z-boson self-energy.

wherein finite-on-shell-mass shifts from (E17) are

$$\delta m_Z^2 = \text{Re} [\Sigma_{finite}^Z (m_Z^2)] \text{ and} \quad (\text{E31})$$

$$\delta m_W^2 = \text{Re} [\Sigma_{finite}^W (m_W^2)] . \quad (\text{E32})$$

In Appendix E 4, we derive  $\Delta r^b$  using stability arguments. Values for squared mass ratios  $\left\{ \frac{\delta m_Z^2}{m_Z^2}, \frac{\delta m_W^2}{m_W^2} \right\}$  and  $\Delta r$  are given in Table II in Appendix F.

Net amplitudes for boson self-energies are finite and satisfy required mass shell conditions (E13) and (E14) for  $b \in \{\gamma, \gamma Z, Z, W\}$ . Amplitude  $\hat{\Sigma}^\gamma$  agrees with the result given in Hollik [19]; however,

$$\left\{ \hat{\Sigma}^{\gamma Z}, \hat{\Sigma}^Z, \hat{\Sigma}^W \right\}$$

including  $\Delta r$  corrections, differ from Hollik's results in two respects:

a) A small finite charge renormalization  $\frac{\alpha}{6\pi} = 3.87 \times 10^{-4}$  from (E22) is absent in  $\left\{ \hat{\Sigma}^Z, \hat{\Sigma}^W \right\}$ , and

b) they include polarization derivative shifts in (E18) — finite parts are given in Appendix F: Table II.

As regards item a), inclusion of any charge renormalization would be inconsistent with the stability approach and result (E27) in particular. For item b), finite parts differ depending on the renormalization scheme, and  $\left\{ \hat{\Sigma}^{\gamma Z}, \hat{\Sigma}^Z, \hat{\Sigma}^W \right\}$  are consistent with the scheme given in [6]; moreover, all four boson self-energies are unified under the same formula (E12). Numerical results for boson polarization functions are given in Appendix F.

## 2. Fermion self-energy corrections

For fermion self-energy corrections, we again expand the core amplitude

$$\Sigma^f(k) = \Sigma^f(m_f) + \left. \frac{\partial \Sigma^f}{\partial k} \right|_{k=m_f} (k - m_f) + H.O.T.. \quad (\text{E33})$$

From (11), the DCM transform is

$$\{m_\kappa\} \rightarrow \{m_\kappa\} \cdot (1 + \lambda\eta) , \quad (\text{E34})$$

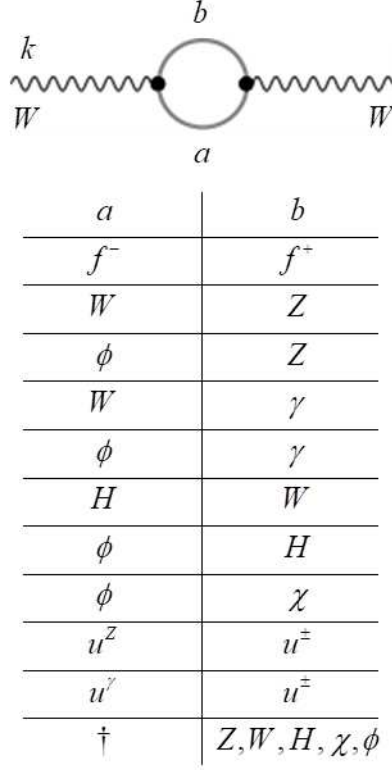


Figure 10. W-boson self-energy.

where the mass set  $\{m_\kappa\} \subseteq \{m_f, m_W, m_Z, \mu\}$  corresponds to terms in (E39). Upon applying (18) to (E33) and noting that  $\{B_i(m_f^2, m_1, m_2); i = 0, 1\}$  occurring in (E39) are invariant under (E34) applied to all mass arguments, we obtain

$$\bar{\Sigma}^f(k) \Big|_{k=m_f} = \Sigma^f(m_f) . \quad (\text{E35})$$

From arguments similar to those for boson self-energies above,  $k - m_f$  and its dimensionless coefficient (first partial) in (E33) are also invariant under (E34). The first partial involves derivatives of  $B_0$  (E5) and  $B_1$  (E6). Finally, higher-order terms in (E33) vanish under (E34), and we have

$$\bar{\Sigma}^f(k) = \Sigma^f(m_f) + \frac{\partial \Sigma^f}{\partial k} \Big|_{k=m_f} (k - m_f) ; \quad (\text{E36})$$

compare with (E11). The net amplitude

$$\hat{\Sigma}^f(k) = \Sigma^f(k) - \bar{\Sigma}^f(k) \quad (\text{E37})$$

satisfies the expected mass shell condition

$$\hat{\Sigma}^f(k) \Big|_{k=m_f} = 0 . \quad (\text{E38})$$

For the corrections shown in Fig. 11, we have [2]

$$\Sigma^f(k) = k \Sigma_V^f(k^2) + k \gamma_5 \Sigma_A^f(k^2) + m_f \Sigma_S^f(k^2) , \quad (\text{E39})$$

where

$$\Sigma_V^f = -\frac{\alpha}{4\pi} \left\{ Q_f^2 [2B_1(k^2; m_f, \mu) + 1] + (v_f^2 + a_f^2) [2B_1(k^2; m_f, m_Z) + 1] + \frac{1}{4s_w^2} [2B_1(k^2; m_f, m_W) + 1] \right\},$$

$$\Sigma_A^f = -\frac{\alpha}{4\pi} \left\{ 2v_f a_f [2B_1(k^2; m_f, m_Z) + 1] - \frac{1}{4s_w^2} [2B_1(k^2; m_f, m_W) + 1] \right\},$$

and

$$\Sigma_S^f = -\frac{\alpha}{4\pi} \{ Q_f^2 [4B_o(k^2; m_f, \mu) - 2] + (v_{i\sigma}^2 - a_{i\sigma}^2) [4B_o(k^2; m_f, m_Z) - 2] \}.$$

Substituting vector ( $V = \not{k}\Sigma_V^f$ ), axial ( $A = \not{k}\gamma_5\Sigma_A^f$ ), and scalar ( $S = m_f\Sigma_S^f$ ) parts of (E39) into (E36), we obtain

$$\bar{\Sigma}^f(k) = \bar{V}(k) + \bar{A}(k) + \bar{S}(k), \quad (\text{E40})$$

where

$$\begin{aligned} \bar{V} &= \not{k}\Sigma_V^f(m^2) + 2m_f^2 \left. \frac{\partial \Sigma_V^f}{\partial k^2} \right|_{k^2=m_f^2} (\not{k} - m_f), \\ \bar{A} &= -\gamma_5 \not{k}\Sigma_A^f(m_f^2), \text{ and} \\ \bar{S} &= m_f \Sigma_S^f(m^2) + 2m_f^2 \left. \frac{\partial \Sigma_S^f}{\partial k^2} \right|_{k^2=m_f^2} (k - m_f). \end{aligned}$$

The identity

$$\frac{\partial \Sigma_J^f}{\partial \not{k}} = 2\not{k} \frac{\partial \Sigma_J^f}{\partial k^2}$$

has been used to evaluate derivatives for  $J = \{V, A, S\}$ . For the derivative of  $A$ , we have replaced  $-\not{k}\gamma_5 = \gamma_5\not{k}$  so  $\not{k}$  stands to the right as required by (E36); one finds

$$\frac{\partial \bar{A}}{\partial \not{k}} = -\gamma_5 \Sigma_A^f,$$

where the symmetrized expression for the derivative

$$\begin{aligned} \frac{\partial}{\partial \not{k}} [\gamma_5 \Sigma_A^f] &= \frac{1}{2} \frac{\partial}{\partial \not{k}} [\gamma_5 \Sigma_A^f + \Sigma_A^f \gamma_5] \\ &= \frac{\partial \Sigma_A^f}{\partial k^2} (\gamma_5 \not{k} + \not{k} \gamma_5) = 0 \end{aligned}$$

has also been employed. Collecting terms, the net amplitude (E37) reduces to

$$\hat{\Sigma}^f(k) = \not{k}\hat{\Sigma}_V(k^2) + \not{k}\gamma_5\hat{\Sigma}_A(k^2) + m_f\hat{\Sigma}_S(k^2), \quad (\text{E41})$$

where

$$\begin{aligned} \hat{\Sigma}_V(k^2) &= \Sigma_V^f(k^2) - \Sigma_V^f(m_f^2) - 2m_f^2 \left. \frac{\partial \Sigma_V^f}{\partial k^2} \right|_{k^2=m_f^2}, \\ \hat{\Sigma}_A(k^2) &= \Sigma_A^f(k^2) - \Sigma_A^f(m_f^2), \\ \hat{\Sigma}_S(k^2) &= \Sigma_S^f(k^2) - \Sigma_S^f(m_f^2) + 2m_f^2 \left. \frac{\partial \Sigma_S^f}{\partial k^2} \right|_{k^2=m_f^2}, \end{aligned}$$

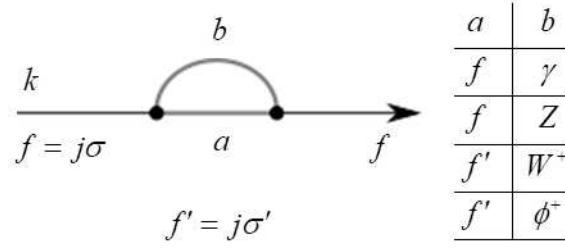


Figure 11. Fermion self-energy.

and  $\Sigma_{VS}^f = \Sigma_V^f + \Sigma_S^f$ .

Using formulae in [2, 19], the renormalization constants are

$$\delta Z_V = -\Sigma_V^f(m_f^2) - 2m_f^2 \left. \frac{\partial \Sigma_{VS}^f}{\partial k^2} \right|_{k^2=m_f^2},$$

$$\delta Z_A = \Sigma_A^f(m_f^2),$$

$$\delta m_f = m_f \Sigma_S^f(m_f^2),$$

and it can be seen that the result (E41) agrees precisely with that obtained from renormalization. Numerical results for fermion self-energy functions for an electron are given in Appendix F: Fig. 17.

### 3. Vertex corrections

Consider the vertex corrections shown in Fig. 12; in the small fermion mass limit [32], only vector and axial vector terms contribute, and the core amplitude is

$$\Lambda_\mu^{\gamma f}(k^2, m_f) = \gamma_\mu \Lambda_V^{\gamma f}(k^2, m_f) - \gamma_\mu \gamma_5 \Lambda_A^{\gamma f}(k^2, m_f), \quad (\text{E42})$$

where  $k^2 = (p' - p)^2$ . The functions

$$\Lambda_{V,A}^{\gamma f}(k^2, m_f) = \Lambda_{V,A}^{\gamma f}(0, m_f) + F_{V,A}^{\gamma f} \left( \frac{k^2}{m_f^2} \right) \quad (\text{E43})$$

involve singular parts at  $k^2 = 0$  and finite form factors  $F_{V,A}^{\gamma f}$  which vanish at  $k^2 = 0$ . Detailed expressions for the functions are given in [19]. Applying (18) and (19), dressed form factors in (E43) vanish as  $\eta \rightarrow \infty$  in

$$m_f(\eta) = m_f(1 + \lambda\eta);$$

therefore,

$$\bar{\Lambda}_\mu^{\gamma f} = \gamma_\mu \Lambda_V^{\gamma f}(0, m_f) - \gamma_\mu \gamma_5 \Lambda_A^{\gamma f}(0, m_f), \quad (\text{E44})$$

and the net vertex amplitude from (17) reduces to the expected result from renormalization

$$\hat{\Lambda}_\mu^{\gamma f} = \gamma_\mu F_V^{\gamma f} \left( \frac{k^2}{m_f^2} \right) - \gamma_\mu \gamma_5 F_A^{\gamma f} \left( \frac{k^2}{m_f^2} \right). \quad (\text{E45})$$

### 4. Wave field renormalization and $\Delta r$ corrections

In the stabilized theory,  $\Delta r$  factors for  $\{W, Z\}$  follow easily from the constancy of the electrical charge; squaring (A16), taking variations

$$\delta e^2 = \delta g_W^2 s_w^2 + g_W^2 \delta s_w^2 = 0 \quad (\text{E46})$$

$$= \delta g_B^2 c_w^2 + g_B^2 \delta c_w^2 = 0, \quad (\text{E47})$$

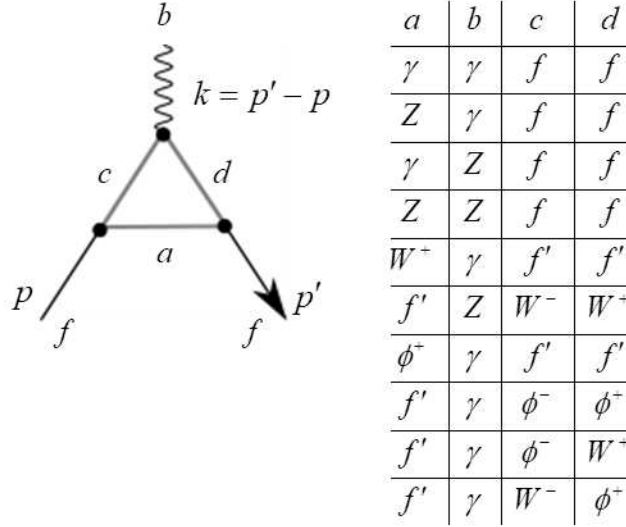


Figure 12. Vertex corrections.

and using (A5), the quadratic coupling deltas are

$$\delta g_W^2 = -g_W^2 \Delta r^W, \quad (\text{E48})$$

$$\begin{aligned} \delta g_Z^2 &= \delta g_W^2 + \delta g_B^2 \\ &= -g_Z^2 \Delta r^Z, \end{aligned} \quad (\text{E49})$$

where

$$\delta g_B^2 = g_B^2 \left( \frac{\delta m_Z^2}{m_Z^2} - \frac{\delta m_W^2}{m_W^2} \right).$$

Therefore, we expect free field propagator modifications of the form

$$\frac{1}{k^2 - m_b^2} \rightarrow \frac{1 - \Delta r^b}{k^2 - m_b^2} \quad (b = W, Z)$$

resulting in small departures of the propagator residue from unity.

For  $\gamma - Z$  mixing, Sirlin's variational method [44] yields a squared mass shift

$$\delta m_{\gamma Z}^2 = -\frac{1}{2} m_Z^2 \Delta r^{\gamma Z}.$$

Using (A8) and defining  $\delta m_{\gamma Z}^2 \equiv \frac{1}{2} \delta g_{\gamma Z}^2 v^2$ , the effective coupling change is

$$\delta g_{\gamma Z}^2 = -g_Z^2 \Delta r^{\gamma Z}. \quad (\text{E50})$$

Standard renormalization theory (SRT) introduces mass and wave field renormalization constants to construct finite S-matrix elements and Green's functions. Renormalized amplitudes are given by [19]

$$\hat{\Sigma}_{ra}^{\gamma} (k^2, \Pi^{\gamma}) = \Sigma^{\gamma} (k^2) + k^2 \delta Z_{\gamma} \equiv k^2 [\Pi^{\gamma} (k^2) + \delta Z_{\gamma}], \quad (\text{E51})$$

$$\hat{\Sigma}_{ra}^{\gamma Z} (k^2, \Sigma^{\gamma Z}) = \Sigma^{\gamma Z} (k^2) + \frac{1}{2} [\delta Z_{\gamma Z} k^2 + \delta Z_{Z\gamma} (k^2 - m_Z^2)], \quad (\text{E52})$$

$$\hat{\Sigma}_{ra}^Z (k^2, \Sigma^Z) = \Sigma^Z (k^2) - \delta M_Z^2 + \delta Z_Z (k^2 - m_Z^2), \quad (\text{E53})$$

$$\hat{\Sigma}_{ra}^W (k^2, \Sigma^W) = \Sigma^W (k^2) - \delta M_W^2 + \delta Z_W (k^2 - m_W^2), \quad (\text{E54})$$

where  $\delta Z_Z$  and  $\delta Z_W$  are displacements of field renormalization constants

$$Z_b = 1 + \delta Z_b \quad (b = Z, W)$$

Table I. Stability and renormalization parameters

Parameter	Stability	Renormalization
$\Sigma^b$	$\hat{\Sigma}_{sa}^b$	$\Sigma^b$
$\delta M_b^2$ ( $b = Z, W$ )	0	$Re [\Sigma^b(m_b^2)]$
$\delta Z_\gamma$	0	$-\Pi^\gamma(0)$
$\delta Z_{Z\gamma}$	0	$\frac{2\Sigma^{\gamma Z}(0)}{m_Z^2}$
$\delta Z_{\gamma Z}$	$2\Delta r^{\gamma Z}$	$\frac{2\Sigma^{\gamma Z}(0)}{m_Z^2} + 2\Delta r^{\gamma Z}$
$\delta Z_Z$	$\Delta r^Z$	$-\Pi^\gamma(0) + \Delta r^Z + \frac{c_w^2 - s_w^2}{s_w c_w} \frac{2\Sigma^{\gamma Z}(0)}{m_Z^2}$
$\delta Z_W$	$\Delta r^W$	$-\Pi^\gamma(0) + \Delta r^W + \frac{c_w}{s_w} \frac{2\Sigma^{\gamma Z}(0)}{m_Z^2}$

from unity, and  $\{\delta Z_{Z\gamma}, \delta Z_{\gamma Z}\}$  define a correction to the  $\gamma - Z$  mixing propagator [30]

$$D_{\mu\nu}^{\gamma Z}(k) = ig_{\mu\nu} \left\{ \frac{1}{2} \left( \frac{\delta Z_{Z\gamma}}{k^2} + \frac{\delta Z_{\gamma Z}}{k^2 - m_Z^2} \right) + \frac{1}{k^2} \Sigma^{\gamma Z}(k^2) \frac{1}{k^2 - m_Z^2} \right\}. \quad (\text{E55})$$

From field renormalization relations

$$W_{\circ\mu} = \left[ Z_W^{1/2} \simeq 1 + \frac{1}{2} \delta Z_W \right] W_\mu,$$

$$B_{\circ\mu} = \left[ Z_B^{1/2} \simeq 1 + \frac{1}{2} \delta Z_B \right] B_\mu,$$

and (A4), the physical fields satisfy

$$\begin{bmatrix} Z_{\circ\mu} \\ A_{\circ\mu} \end{bmatrix} = \begin{bmatrix} 1 + \frac{1}{2} \delta Z_Z & \frac{1}{2} \delta Z_{Z\gamma} \\ \frac{1}{2} \delta Z_{\gamma Z} & 1 + \frac{1}{2} \delta Z_\gamma \end{bmatrix} \begin{bmatrix} Z_\mu \\ A_\mu \end{bmatrix},$$

where subscript "o" denotes bare, as opposed to renormalized quantities, and renormalization constants satisfy [39]

$$\begin{bmatrix} \delta Z_Z \\ \delta Z_\gamma \end{bmatrix} = \begin{bmatrix} c_w^2 & s_w^2 \\ s_w^2 & c_w^2 \end{bmatrix} \begin{bmatrix} \delta Z_W \\ \delta Z_B \end{bmatrix},$$

$$\delta Z_{Z\gamma} = -s_w c_w (\delta Z_W - \delta Z_B) - \Delta r^{\gamma Z}, \text{ and}$$

$$\delta Z_{\gamma Z} = -s_w c_w (\delta Z_W - \delta Z_B) + \Delta r^{\gamma Z}.$$

Ordinarily, the core amplitude  $\Sigma^b$  is used in (E51)–(E54); however, with the stabilized amplitudes at our disposal, we are free to replace  $\Sigma^b$  with  $\hat{\Sigma}_{sa}^b = \hat{\Sigma}^b$  from (E16) to easily determine all renormalization constants. Applying mass shell renormalization (stability) conditions

$$\begin{bmatrix} \hat{\Pi}_{ra}^\gamma(0, \hat{\Pi}_{sa}^\gamma) \\ \hat{\Sigma}_{ra}^{\gamma Z}(0, \hat{\Sigma}_{sa}^{\gamma Z}) \\ \hat{\Sigma}_{ra}^Z(m_Z^2, \hat{\Sigma}_{sa}^Z) \\ \hat{\Sigma}_{ra}^W(m_W^2, \hat{\Sigma}_{sa}^W) \end{bmatrix} = \vec{0},$$

only finite wave field stability corrections for  $\Delta r$  shown in Table I are non-zero; values for renormalization constants from SRT are included for comparison.

Referring to (E55), the stability result  $\delta Z_{Z\gamma} = 0$  means that the photon propagator has no  $Z$ -component

$$\frac{\delta Z_{Z\gamma}}{k^2} = 0;$$

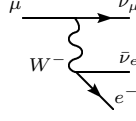
consequently, there is no direct coupling between the photon and a neutral current  $J_{NC}$  for  $\gamma - Z$  mixing — not even an infinite one! On the other hand, an electromagnetic current couples to  $J_{NC}$  via the  $Z$  with amplitude

$$\frac{1}{2} \delta Z_{\gamma Z} = \Delta r^{\gamma Z}$$

as is well known and suggested by (E50) above.

## 5. Muon decay and $\Delta r$ corrections

In the Born approximation, the muon decay amplitude corresponds to a Feynman diagram



in the Standard Model. The resulting decay rate [19]

$$\Gamma_\mu^\circ = \frac{\alpha^2}{384\pi} \frac{m_\mu^5}{s_w^4 m_W^4} \left(1 - \frac{8m_e^2}{m_\mu^2}\right),$$

when reconciled with the Fermi contact model prediction

$$\Gamma_\mu^F = \frac{G_F^2 m_\mu^5}{192\pi^3} \left(1 - \frac{8m_e^2}{m_\mu^2}\right),$$

yields the Fermi constant in lowest order

$$G_F^\circ = \frac{\pi\alpha}{\sqrt{2}s_w^2 m_W^2}. \quad (\text{E56})$$

With higher-order QED corrections [28, 38],

$$\frac{1}{\tau_\mu} = \frac{G_F^2 m_\mu^5}{192\pi^3} f\left(\frac{m_e^2}{m_\mu^2}\right) (1 + \Delta_{QED})$$

defines  $G_F$  in terms of the precisely measured muon lifetime  $\tau_\mu$ , where

$$f(x) = 1 - 8x - 12x^2 \ln x + 8x^3 - x^4, \text{ and} \\ \Delta_{QED} = \frac{\alpha}{2\pi} \left(\frac{25}{4} - \pi^2\right) + O(\alpha^2).$$

In addition to the one-loop correction shown in  $\Delta_{QED}$ ,  $O(\alpha^2)$  corrections for two-loops are also known [31, 37, 45]. These QED corrections involve several renormalization schemes; however, the corresponding stabilized QED corrections are finite without renormalization as shown in Appendix C. Stability corrections for vacuum polarization involve a subtraction of the form (C3) at  $k^2 = 0$  and are therefore equivalent to the on-shell renormalization scheme. For other renormalization schemes; for example, the modified minimal subtraction  $\overline{MS}$ ,  $\Delta_{QED}$  involves a coupling constant renormalization. Ritbergen [37] gives a prescription

$$\alpha(m_\mu) = \frac{\alpha}{1 - \frac{\alpha}{3\pi} \ln \frac{m_\mu^2}{m_e^2}} + O(\alpha^3) \quad (\text{E57})$$

relating the  $\overline{MS}$  coupling constant  $\alpha(m_\mu)$  to the on-shell (experimental) value  $\alpha$  [47]. However, from (C7) and (E27), the stabilized results are unique, and the prescription (E57) does not represent an intrinsic renormalization of electrical charge in the stabilized theory.

Electroweak corrections to the muon lifetime involve  $\Delta r$  corrections to the Fermi constant [18, 19, 44]

$$G_F = G_F^\circ [1 + \Delta r], \quad (\text{E58})$$

where after renormalization

$$\Delta r = -\Delta r^W - \frac{\delta m_W^2}{m_W^2} + \frac{\hat{\Sigma}^w(0)}{m_W^2} + \Delta r^{\text{[vertex, box]}}, \quad (\text{E59})$$

where

$$\Delta r^{\text{[vertex, box]}} = \frac{\alpha}{4\pi s_w^2} \left(6 + \frac{7 - 4s_w^2}{2s_w^2} \ln c_w^2\right).$$



Table II. Numerical results for  $\Delta r$  and derivative shifts.

Item	$\gamma$	$\gamma Z$	$Z$	$W$
$m_b$ ( $GeV/c^2$ )	0	$\{0, m_Z\}$	91.1876	80.379
$\frac{\delta m_b^2}{m_b^2}$	-	-	-0.1061	-0.0920
$\Delta r^b$	0	0.0258	-0.0329	-0.0470
$\left. \frac{\partial \Sigma^b}{\partial s} (m_b^2) \right _{finite}$	$-\frac{\alpha}{6\pi}$	0.001165	-0.1142	-0.1252

From a stability perspective, the first two terms of (E59) are due to finite mass shifts (E31) and (E32); taking into account (E27), variation of (E56) yields

$$\delta G_F^c = -G_F^c \left[ \Delta r^W + \frac{\delta m_W^2}{m_W^2} \right]. \quad (\text{E60})$$

In standard renormalization theory, divergent bare parameters  $\{\alpha_o, s_w^o, m_w^o\}$  replace those in (E56), and the expression for  $\Delta r$  includes a charge renormalization term  $\delta\alpha_o$  which is subsequently incorporated into a renormalized coupling.

### Appendix F: Numerical results

Values for  $\Delta r$  are tabulated in Table II using  $\sin^2(\theta_W) = 0.23122(4)$  and other physical constants [47].

Real parts of boson polarization functions (E18) are plotted in Figs. 13–16. Stability profiles use amplitudes (E12) or, equivalently, (E16) exclusive of  $\Delta r$ . Results in Fig. 13 agree with those in Fig. 8 of [2] notwithstanding updated physical constants [47]; QED results are added for comparison using an analytic result for (C3) given in [26]. For numerical evaluation of photon self-energy and  $\gamma-Z$  mixing profiles shown in Figs. 13–14, the stability value at  $s = 0$  is not represented; but analytically,  $\hat{\Pi}^\gamma(0) = \hat{\Pi}^{\gamma Z}(0) = 0$  from (E18). Differences between "Stability +  $\Delta r$ " profiles shown in Figs. 14–16 and Figs. 9–11 of [2] are due to

1.  $\Delta r$  impacts arising from updates to  $\{\Sigma^Z, \Sigma^W\}$  in [19] relative to [2],
2. derivative shifts in Table II, and
3. updated physical constants including a Higgs mass measurement  $125.18 \pm 0.16 GeV/c^2$  [47].

Analytic expressions for  $F(s, m_1, m_2)$  given in [2] and its partials were verified against numerical integration results for all mass arguments  $m_1$  and  $m_2$  over the range  $0 < \sqrt{|k^2|} < 200 GeV$ .

Electron self-energy function profiles  $\{\hat{\Sigma}_V, \hat{\Sigma}_A, \hat{\Sigma}_S\}$  shown in Fig. 17 agree with those in Fig. 18a of [2].

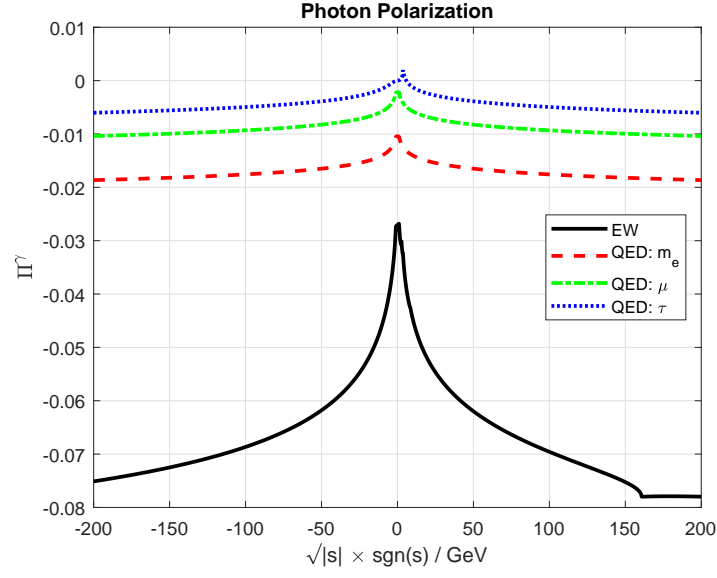


Figure 13. Stabilized electroweak photon polarization is compared with QED for electron, muon, and tau.

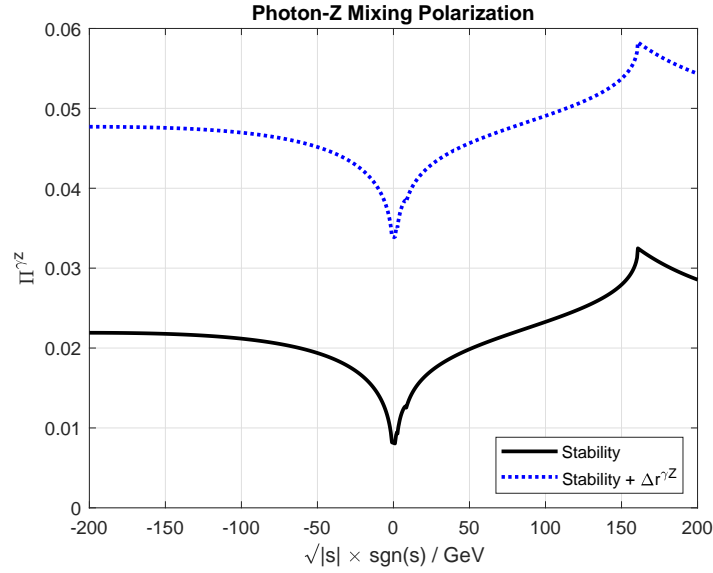


Figure 14. Stabilized photon-Z mixing profiles with/without adjustments for  $\Delta r$ .

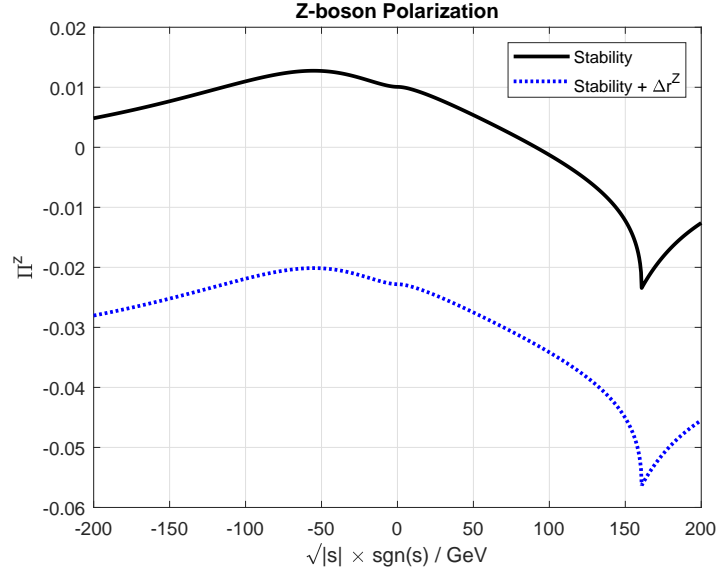


Figure 15. Stabilized Z–boson polarization profiles with/without adjustments for  $\Delta r$ .

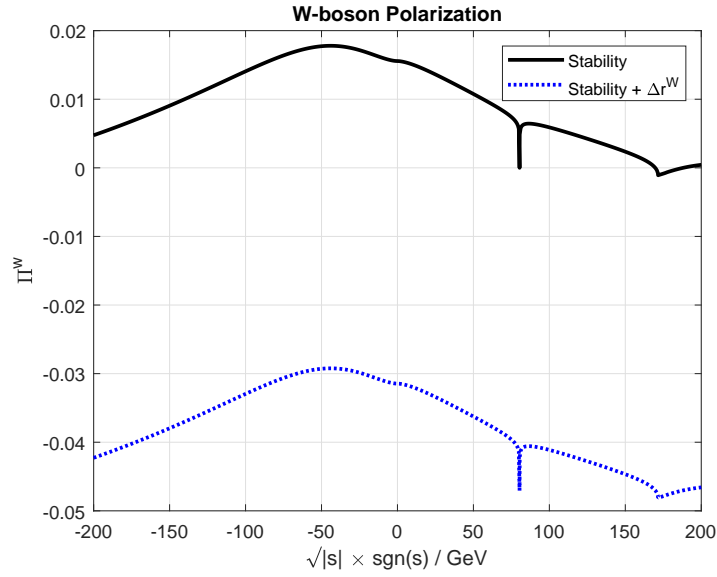


Figure 16. Stabilized W–boson polarization profiles with/without adjustments for  $\Delta r$ .

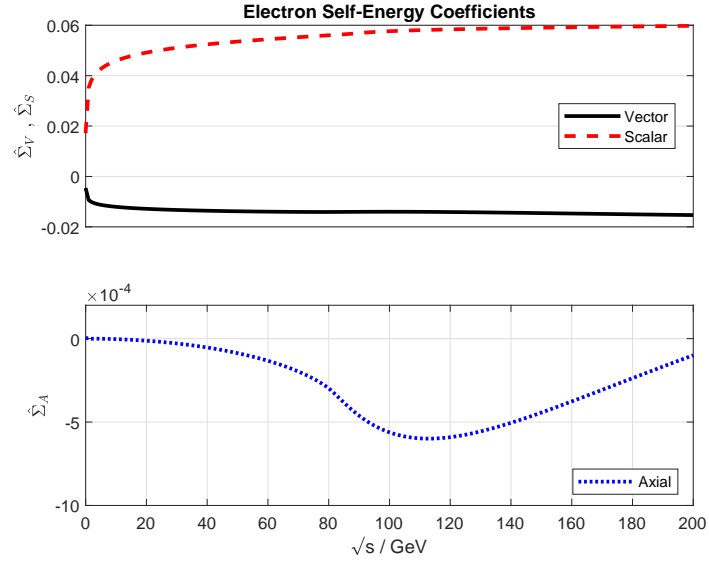


Figure 17. Electron self-energy coefficients for vector, axial, and scalar contributions.

- 
- [1] Bjorken, J. D., and S. D. Drell (1964), *Relativistic Quantum Mechanics* (McGraw-Hill, New York) p. 163.
- [2] Böhm, M., H. Spiesberger, and W. Hollik (1986), *Fortschritte Der Physik* **34** (11), 687.
- [3] Callan, C. G. (1970), *Phys. Rev. D* **2**, 1541.
- [4] Chlouber, C. D. (2021), “Stabilized quantum field theory,” Vixra preprint.
- [5] Cutkosky, R. E. (1960), *J. Math. Phys.* **1** (5), 429.
- [6] Denner, A. (1993), *Fortschr. Phys.* **41**, 307.
- [7] Dissertori, G. (2016), “The determination of the strong coupling constant,” Chap. 6 (The Standard Theory of Particle Physics) pp. 113–128.
- [8] Dyson, F. J. (1949), *Phys. Rev.* **75** (3), 486.
- [9] Dyson, F. J. (1949), *Phys. Rev.* **75**, 1736.
- [10] Feynman, R. P. (1949), *Phys. Rev.* **76** (6), 769.
- [11] Feynman, R. P. (1949), *Phys. Rev.* **76** (6), 749.
- [12] Foley, H. M., and P. Kusch (1948), *Phys. Rev.* **73** (4), 412.
- [13] Gell-Mann, M., M. L. Goldberger, and W. Thirring (1954), *Phys. Rev.* **95**, 1612.
- [14] Glashow, S. L. (1961), *Nucl. Phys. B* **22**, 579.
- [15] Gross, D. J., and F. Wilczek (1973), *Phys. Rev. D* **8**, 3633.
- [16] Gross, D. J., and F. Wilczek (1973), *Phys. Rev. Lett.* **30**, 1343.
- [17] Higgs, P. W. (1964), *Phys. Rev. Lett.* **13**, 508.
- [18] Hollik, W. (2006), *Journal of Physics: Conference Series* **53**, 7.
- [19] Hollik, W. F. (1990), *Fortschr. Phys.* **38** (3), 165.
- [20] 't Hooft, G. (1971), *Nucl. Phys. B* **35**, 167.
- [21] 't Hooft, G., and M. Veltman (1972), *Nucl. Phys. B* **50**, 318.
- [22] 't Hooft, G., and M. Veltman (1972), *Nucl. Phys. B* **44** (1), 189.
- [23] 't Hooft, G., and M. Veltman (1979), *Nucl. Phys. B* **153**, 365.
- [24] Jauch, J. M., and F. Rohrlich (1976), *The Theory of Photons and Electrons* (Springer-Verlag, New York) Ch. 9-10, App. A5-2, Supp. S2.
- [25] Källén, G. (1952), *Helv. Phys. Acta.* **25**, 417.
- [26] Källén, G. (1972), *Quantum Electrodynamics* (Springer-Verlag, New York) p. 149.
- [27] Källén, G., and A. Sabry (1955), *Dan. Mat. Fys. Medd.* **29** (17), 1.
- [28] Kinoshita, T., and A. Sirlin (1959), *Phys. Rev.* **113** (6), 1652.
- [29] Mandl, F., and G. Shaw (1984), *Quantum Field Theory* (Wiley, New York) pp. 188, 227, 231.
- [30] Nagashima, Y. (2013), *Elementary Particle Physics: Foundations of the Standard Model*, Vol. 2 (Wiley) Sec. 5.2.2.
- [31] Pak, A., and A. Czarnecki (2008), *Phys. Rev. Lett.* **100** (24), 241807.
- [32] Passarino, G., and M. Veltman (1979), *Nucl. Phys. B* **160** (1), 151.
- [33] Peskin, M. E., and D. V. Schroeder (1995), *An Introduction to Quantum Field Theory* (Addison-Wesley, New York) p. 332ff, Sec. 16, A.4.
- [34] Poincaré, H. (1906), *Rendiconti del Circolo Matematico di Palermo* (1884-1940) **21** (1), 129.
- [35] Politzer, H. D. (1973), *Phys. Rev. Lett.* **30**, 1346.
- [36] Politzer, H. D. (1974), *Physics Reports* **14** (4), 129.
- [37] van Ritbergen, T., and R. G. Stuart (2000), *Nucl. Phys. B* **564**, 343.
- [38] Roos, M., and A. Sirlin (1971), *Nucl. Phys. B* **29** (1), 296.
- [39] Ross, D. A., and J. C. Taylor (1973), *Nucl. Phys. B* **51**, 125.
- [40] Salam, A. (1951), *Phys. Rev.* **82** (2), 217.
- [41] Salam, A. (1968), in *Elementary Particle Theory*, edited by N. Svartholm (New York : Wiley – Stockholm : Almqvist and Wiksell).
- [42] Schweber, S. S., H. A. Bethe, and F. de Hoffmann (1955), *Mesons and Fields*, Vol. I (Row, Peterson and Co.) Ch. 21a discusses H. A. Kramer’s mass renormalization principle. See Ch. 21e for polarization tensor factorization.
- [43] Schwinger, J. (1948), *Phys. Rev.* **73** (4), 416.
- [44] Sirlin, A. (1980), *Phys. Rev. D* **22**, 971.
- [45] Steinhauser, M., and T. Seidensticker (1999), *Phys. Lett. B* **467**, 271.
- [46] Symanzik, K. (1970), *Commun. Math. Phys.* **18**, 227.
- [47] Tanabashi, M., *et al.* (2018), *Phys. Rev. D* **98** (3), 030001.
- [48] Ward, J. C. (1951), *Proc. Phys. Society* **A64**, 54.
- [49] Weinberg, S. (1960), *Phys. Rev.* **118** (3), 838.
- [50] Weinberg, S. (1967), *Phys. Rev. Lett.* **19**, 1264.
- [51] Weisskopf, V. F. (1934), *Z. Angew. Phys.* **89**, 27, english translation given in A. I. Miller, *Early Quantum Electrodynamics: A Source Book* (Cambridge U. Press, New York, 1994).